REPUBLIC OF TURKEY

YILDIZ TECHNICAL UNIVERSITY GRADUATE SCHOOL OF NATURAL AND APPLIED SCIENCES

MICROWAVE DEVICE MODELLING USING NOVEL ALGORITHMS

Aysu BELEN

DOCTOR OF PHILOSOPHY THESIS Department of Electronics and Communications Engineering Communication Program

Advisor

Prof. Dr. Filiz GÜNEŞ

Co-Advisor

Assoc. Prof. Dr. Peyman MAHOUTI

February, 2021

REPUBLIC OF TURKEY

YILDIZ TECHNICAL UNIVERSITY

GRADUATE SCHOOL OF NATURAL AND APPLIED SCIENCES

MICROWAVE DEVICE MODELLING USING NOVEL ALGORITHMS

A thesis submitted by Aysu BELEN in partial fulfillment of the requirements for the degree of DOCTOR OF PHILOSOPHY is approved by the committee on 09.02.2021 in Department of Electronics and Communication Engineering, Communication Program.

Prof. Dr. Filiz GÜNEŞ Assoc. Prof. Dr. Peyman MAHOUTI Yıldız Technical University İstanbul Cerrahpaşa University Advisor Co-Advisor **Approved By the Examining Committee** Prof. Dr. Filiz GÜNEŞ, Advisor Yıldız Technical University Prof. Dr. Ahmet KIZILAY, Member Yıldız Technical University Doç. Dr. Nihan KAHRAMAN, Member Yıldız Technical University Prof. Dr. Fikret GÜRGEN, Member Boğaziçi University Prof. Dr. Ahmet Arif ERGİN, Member Yeditepe University

I hereby declare that I have obtained the required legal permissions during data collection and exploitation procedures, that I have made the in-text citations and cited the references properly, that I haven't falsified and/or fabricated research data and results of the study and that I have abided by the principles of the scientific research and ethics during my Thesis Study under the title of Microwave Device Modelling using Novel Algorithms supervised by my supervisor, Prof. Dr. Filiz GÜNEŞ. In the case of a discovery of false statement, I am to acknowledge any legal consequence.

Aysu BELEN

Signature

This study was supported by the Council of Higher Education (YÖK) Grant No: YOK 100/2000 PhD Scholarsahip. This study was supported by the Scientific and Technological Research Council of Turkey (TUBITAK) Grant No: 2211-A.

Dedicated to my family and my husband

ACKNOWLEDGEMENTS

I wish to express my sincere appreciation to my advisor, Prof. Dr. Filiz GÜNEŞ, for constant support, precious scientific discussions, providing me an excellent working environment and helping me to have better perspective in my scientific thinking throughout my doctorate. She will always be in my memories as a very kind and splendid personality.

I also wish to express my sincere thanks to Prof. Dr. Ahmet KIZILAY and Prof. Dr. Fikret GÜRGEN for serving on my thesis committee. I highly appreciate their interest in my study as well as their precious comments and questions.

I would like to thank the Council of Higher Education (YÖK) for supporting me with YOK 100/2000 PhD Scholarsahip and Scientific and Technological Research Council of Turkey (TUBITAK) for supporting me with 2211/A doctoral scholarship during my PhD education.

I would like to offer my special thanks to my co-advisor, Assoc. Prof. Dr. Peyman MAHOUTI for his guidance, encouragement during my thesis. I deeply thank him for helping me in understanding the theoretical concepts of optimization techniques as well as the computer applications. And also he always helped me whenever I was in need. I am very grateful to him.

I am very grateful to my husband, Mehmet Ali BELEN for his endless emotional support and understanding during my doctoral dissertation. I offer my special thanks to him for his all support and help.

None of this would have been possible without the prayers, support and encouragement of my parents. I owe them everything. Their continuous prayers have always given me a hidden support and confidence. I offer my special thanks to them for their all support and help.

Aysu BELEN

TABLE OF CONTENTS

LIST (OF SYM	IBOLS	viii
LIST (OF ABE	BREVIATIONS	X
LIST (OF FIG	URES	xii
LIST (OF TAE	BLES	xii xiv xv xvii 1 n for Intelligence Transportation Systems
ABST	RACT		
ÖZET			xvii
1 IN7	ΓRODU	ICTION	1
1.1	Litera	ture Review	1
	1.1.1	Antenna Design for Intelligence Transportation Systems	1
	1.1.2	Artifical Intelligence Based Algorithms	8
	1.1.3	Meta-Heuristic Optimization	8
	1.1.4	Artifical Neural Network	8
	1.1.5	3D Printing Technology	9
1.2	Objec	tive of the Thesis	10
1.3	Hypot	thesis	10
2 TR	AVELII	NG WAVE ANTENNA	12
2.1	Micro	strip Tapered Traveling Wave Antenna for Wide Range of Beam	
	Scanr	ning in X- and Ku- Bands	12
	2.1.1	Design and Simulation of Microstrip Tapered TWA	13
	2.1.2	Experimantal Results	19
	2.1.3	Discussion on Performance of Proposed TWA	22
3 (11)	RSTRA	TE INTEGRATED WAVEOUIDE ANTENNA	24

	3.1	Desig	n Optimization of a Dual- Band Microstrip SIW antenna Using	
		Differ	rential Evolutionary Algorithm for X- and K- Band Radar Applicatio	ns
				24
		3.1.1	Desgin Optimization of Dual-Band SIW Antenna Using DEA	25
		3.1.2	Discussion on Performance of Proposed SIW Antenna Design	32
4	MU	ILTILA	YER DIELECTRIC LENS ANTENNA	34
	4.1		vel Design of High Performance Multilayered Cylindrical Dielectric Antenna Using 3D Printing Technology	34
		4.1.1	Design of Multilayered Cylindrical Dielectric Lens	34
		4.1.2	3D Printing Fabrication and Experimental Results of MLCDLA	40
		4.1.3	Discussion on Performance of Proposed MLCDLA	43
5	RE	FLECT	ARRAY ANTENNA	45
	5.1		inted Wideband Flat Gain Multilayer Non-Uniform Reflectarray	45
		5.1.1	Design Process Unit Cell Modelling	45
		5.1.2	Optimum MNURA Unit Cell	50
		5.1.3	Simulated and Measured Results	52
		5.1.4	Discussion on Performance of Proposed MNURA Design	57
6	RES	SULTS	AND DISCUSSION	58
R	EFEI	RENCE	S	61
D	IIDI	I <i>C</i> ATIO	ON EDOM THE THESIS	72

LIST OF SYMBOLS

dB	Decibel
μ	Dielectric Permeability
ε	Dielectric Permittivity
\mathcal{E}_{e}	Effective Dielectric Permittivity
7	Focal Distance of Feed Antenna
λ_0	Free Space Wavelength
f	Frequency
m	Length of the Patch
δ	Loss Angle
M	Number of Divisions in x-Direction
N	Number of Division in y-Direction
k	Propagation Constant in the Medium
γ_{g}	Propagation Constant in Waveguide
\mathcal{E}_r	Relative Dielectric Constant of the Substrate
f_r	Resonance Frequency
c	Speed of Light in Free Space
η_s	Spillover Efficiency
h	Substrate Thickness
$\eta_{\scriptscriptstyle t}$	Taper Efficiency

 $Tan\delta$ Tangent Loss t Thickness

 λ_r Wavelength in the Substrate

D Vertical Edge Size of Array Surface

LIST OF ABBREVIATIONS

ANN Artificial Neural Network

BPMLP Back Propagation Multi-Layer Perceptron

BPNN Back Propagation Neural Network

CAD Computer Aided Design

CST Computer Simulation Technology

DBM Digital Beam Melting

DEA Differential Evolutionary Algorithm

DMLS Direct Metal Laser Sintering

DRA Dielectric Resonator Antennas

EA Evolutionary Algorithm

EXT Extrapolation

FDM Fused Deposition Modelling

FDTS Feasible Design Target Space

FEN Function of Evolution Number

FSS Frequency Selective Surface

GA Genetic Algorithm

GPS Global Position System

GRNN Generalized Regression Neural Network

INT Interpolation

ISM Industrial Scientific Medical Band

IOT Internet of Things

ITS Intelligent Transportation Systems

LOM Laminated Object Manufacturing

M2M Machine to Machine

MAE Mean Absolute Error

ML Machine Learning

MLP Multilayer Perceptron

MNURA Multi-layer Non-Uniform Reflect-Array

NN Neural Networks

PBC Periodic Boundary Condition

PSO Particle Swarm Optimization

RA Reflectarray Antenna

RCS Radar Cross Section

RF Radio Frequency

RME Relative Mean Error

RMSE Root Mean Square Error

SIW Substrate-Integrated Waveguide

SiP System in Packet

SLM Selective Laser Melting

SLL Side Lobe Level

SLS Selective Laser Sintering

SoS System on- Substrate

SRM Structural Risk Minimization

SVs Support Vectors

SVM Support Vector Machines

SVRM Support Vector Regression Machines

TEM Transverse Electromagnetic

TWA Traveling Wave Antennas

UWB Ultra-wide Band

LIST OF FIGURES

Figure 1.1	Typical RA Unit Elements with Phase Compensation Reflection w.r.t Variable (a) Transmission Line Lengths, (b) Dipoles' and Rings' Sizes, (c) Patch's Size, (d) Elements' Rotations[3]5
Figure 1.2	A Traditional RA Design with the Feeding [69]6
Figure 1.3	A Traditional Large Scale Planar RA with Variable Stub Length Patch Element [69]7
Figure 2.1	(a) An Example for a TWA Design (Beverage antenna) [125] (b) Basic Shapes of the Travelling Wave Antennas [45]14
Figure 2.2	(a) Unit Cell Design (b) Traditionally Resistive Loaded Travelling Wave Antenna Design14
Figure 2.3	The Proposed PLTWA
Figure 2.4	Simulated (a) Return Loss (b) Maximum Gain (c) Efficiency of TWA Design17
Figure 2.5	Simulated Radiation Pattern of PLTWA for Variant Frequencies 18
Figure 2.6	Fabricated PLTWA19
Figure 2.7	Simulated and Measured S ₁₁ of PLTWA20
Figure 2.8	Measured Gain and Beam Scanning with Frequency21
Figure 2.9	Measured Radiation Pattern for Variant Frequencies21
Figure 3.1	Parametric Layout of SIW Antenna24
Figure 3.2	Flow Chart of the SIW Antenna Design Optimization26
Figure 3.3	Fabricated Antenna
Figure 3.4	Simulated Gain Patterns (a) 12GHz, (b) 24 GHz29
Figure 3.5	Simulated and Measured Return Losses
Figure 3.6	Measured Far Field Gain
Figure 4.1	Schematic and Geometrical Structure of the Proposed MLCDLA 35
Figure 4.2	Simulated S_{11} Analysis of Different Cases
Figure 4.3	Simulated Gain Analysis of Different Cases
Figure 4.4	Simulated Radiation Patterns of Case 1
Figure 4.5	Simulated E-field Distribution at (a) 8 GHz, (b) 10 GHz, (c) 12 GHz 39
Figure 4.6	Fabricated MLCDLA Model40
Figure 4.7	Simulated and Measured S ₁₁ 41

Figure 4.8	Maximum Gain Over the Operation Band42
Figure 4.9	Measured Radiation Patterns of MLCDLA for $^\phi$ =90° at (a) 8 GHz, (b) 10 GHz, (c) 12 GHz42
Figure 5.1	Unit Cell Structure of the MNURA h ₁ , h ₂ 46
Figure 5.2	Black Box Model of the MNURA Unit Element46
Figure 5.3	Reflection Phase Variations of MNURA Unit Element with (a) h_1 [h_2 =10mm, ϵ_r =2, f =10GHz], (b) h_2 [h_1 =10mm, ϵ_r =2, f =10GHz], (c) ϵ_r [h_1 =10mm, h_2 =10mm, f =10GHz], (d) f [h_1 =10mm, h_2 =10mm, ϵ_r =2] 49
Figure 5.4	(a) 3D View, (b) Radiation Pattern @10 GHz of the 20x20 MNURA Antenna
Figure 5.5	Simulated (a) Return Loss (b) Radiation Patterns53
Figure 5.6	Prototyped 3D Printed NURA54
Figure 5.7	Measured NURA S ₁₁ Characteristic55
Figure 5.8	Measured Radiation Pattern of 3D Printed MNURA at (a) 8 GHz, (b) 10 GHz, (c) 12 GHz56

LIST OF TABLES

Table 2.1 Parameter List of PLTWA Design in mm	16
Table 2.2 Simulated Performance Comparisons of Resistive Loaded TV PLTWA	
Table 2.3 Sample Table Measured Performance of PLTWA	20
Table 2.4 Comparison of PLTWA with counterpart designs in literature	22
Table 3.1 Constraints of the Variables in (mm)	25
Table 3.2 Performance Results of DEA*	27
Table 3.3 Number of Function Evaluations of DEA*	28
Table 3.4 Optimal Parameter List in (mm)	28
Table 3.5 Comparison of the Realized Gains	31
Table 3.6 Comparison of Antenna with Literature	32
Table 4.1 Parameter values of the fabricated lens case 1	
Table 4.2 Parameter values for parametric analysis	36
Table 4.3 Simulated and measured radiation characteristics of the production MLCDLA	roposed
Table 4.4 Comparison of Gain (dBi) Enhancements of the Typical Horn Mo the Similar Bandwidth	
Table 5.1 Variables of the MNURA Unit element	46
Table 5.2 User defined parameters of MLP NN algorithms	47
Table 5.3 Performances of the MLP NN MODELS for 10 runs based on the t set	
Table 5.4 H ₁ values of quadratic MNURA in (mm)	51
Table 5.5 Simulation results of MNURA antenna design	53
Table 5.6 Performance comparison of the proposed MNURA with cour designs in literature	•

Microwave Device Modelling using Novel Algorithms

Aysu BELEN

Department of Electronic and Communication Engineering Doctor of Philosophy Thesis

Advisor: Prof. Dr. Filiz GÜNEŞ

Co-advisor: Assoc. Prof. Dr. Peyman MAHOUTI

Intelligence Transportation Systems (ITS) is a research field in which researchers study methods and solutions to overcome problems of transportation systems in an environment friendly, low cost, and sustainable ways to reach maximum efficiency in transportation systems. The main aim of the studies of ITS is to reduce the work load of human personnel and possible human mistakes during all operation process. Todays, by means of the developments in ITS, their applications become widespread. Today many vehicles are actively using Global Position System (GPS), Wireless network communication (Wi-Fi, WiMAX, WiBro) or mobile networks (4G, 4.5G, 5G, LTE), RF or IR waves etc. are being used for machine to machine or machine- person communications, where one of the main constituents is availability of the high performance antennas. In fact, with the ever increasing need of technology and complexity of systems and their environment, need of high performance microwave antenna designs are also increased. This encourages microwave engineers to study for novel methods of modelling and prototyping to meet the high demands of communication industry.

In this thesis, it was aimed at proposing novel design methodologies and technologies to meet the current unfilled antenna demands for Intelligence Transportation Systems. Thus four different types of antenna were studied:

- I. Patch Loaded Traveling Wave Antenna (PLTWA),
- II. Microstrip SIW antenna,
- III. Multilayer dielectric loaded lens antenna,
- IV. A large scale Reflectarray antenna with flat gain characteristics.

Design stages and realizations of these antennas can briefly be summarized as follows: Firstly the antenna models are built up either by using 3D EM simulation tools or by Artificial Neural Network (ANN)s trained by the data sets created via 3D EM simulation tools, then these models are utilized via meta-heuristic optimization algorithms in the design stage to be ready in the realization where prototypes are produced using 3D printing technology as high performance and low cost antennas. Finally measurements have also been made for the comparison of the theoretical and experimental performance of the prototype antennas to be sure for the target to be realized. As conclusion we are glad to present our novel antenna designs in use of communication industry including Intelligence Transportation Systems to meet their current unfilled demands.

Keywords: Microwave, antenna, microstrip antenna, reflectarray, beam scaning, substrate integrated wavequide, lens antenna, intelligence transportation systems.

VII DIZ TECHNICAL HNIVEDCITY

Yenilikçi Algoritmalar Kullanılarak Mikrodalga Cihaz Tasarımı

Aysu BELEN

Elektronik ve Haberleşme Mühendisliği Anabilim Dalı Doktora Tezi

Danısman: Prof. Dr. Filiz GÜNES

Eş-Danışman: Doç. Dr. Peyman MAHOUTI

Akıllı ulaşım sistemleri (AUS) araştırmacıların, çevre dostu, düşük maliyetli ve de sürdürülebilir bir çözüm yöntemini geliştirerek taşımacılıktaki problemleri giderme ve taşımacılıktaki sistem verimini maksimize etmeye odaklanmış bir araştırma konusudur. AUS'deki ana amaç olası insan hatalarını ve de insanlara ait bütün operasyon anlarındaki iş yükünü azaltmaktır. Günümüzde birçok araç aktif bir şekilde Küresel Konumlama Sistemi (GPS), Kablosuz Haberleşme sistemleri (Wi-Fi, WiMAX, WiBro), mobil ağları (4G, 4.5G, 5G, LTE), veya RF, IR dalgalarını kullanarak Makine-Makine ve/veya makine-insan haberleşmesini yapmaktadırlar.

Sürekli artan teknoloji ve çevre ihtiyaçları ve bunlara bağlı artan karmaşık sistemler, yeni nesil yüksek performans mikrodalga anten tasarımlarına olan ihtiyacı da artırmıştır. Buda mikrodalga mühendislerinin endüstrinin bu yüksek taleplerini çözmek için yeni nesil, modelleme ve üretim metotlarının geliştirmesi için cesaretlendirmistir.

Bu tezde, çeşitli anten tasarımlarının yenilikçi metotlar ile tasarımı yapılarak, AUS'nin ihtiyaç duyduğu yüksek performansı yapıların tasarımı hedeflenmiştir. Burada, 4 farklı anten yapısı incelemeye alınmıştır;

xviii

- I. Yama Yüklü Yürüyen Dalga Anten,
- II. SIW (Substrate Integrated Wavequide) mikroşerit yama anten,
- III. Çok katlı dielektrik lens yüklü anten,
- IV. Düz Kazanç karakteristiğine sahip büyük ölçekli yansıtıcı dizi anten.

Bu bahsi edilen anten yapılarının tasarım aşamaları kısaca şu şekilde özetlenebilinir: öncelikle anten yapıları 3B benzim araçları ve/veya bu araçlardan oluşturulan veriler ile eğitilmiş olan Yapay Sinir Ağları ile modellenmeleri, daha sonrasında ise yenilikçi meta-sezgisel algoritmalar desteği ile tasarım optimizasyonlarının gerçekleştirilmesi. 3B yazıcı teknolojisi kullanılarak tasarım optimizasyonu yapılmış devrelerin maliyetinin düşürülmesi. Son olarak ise ölçümler ve elde edilen veriler literatürde var olan rakip ve benzer çalışmalar ile kıyaslanması yapılmıştır. Sonuç olarak, 3B Simulator araçları, Yapay Sinir ağları ve meta-sezgisel optimizasyon gibi Yapay Zeka tabanlı Algoritmalar, ve 3B yazıcı teknolojisi kullanılarak, performansı yüksek, düşük maliyete sahip AUS uygulamalarına yönelik uygun anten modelleri geliştirilmiştir.

Anahtar Kelimeler: Mikrodalga, anten, mikroşerit anten, yansıtıcı dizi, hüzme tarama, lens anten, akıllı ulaşım sistemleri.

YILDIZ TEKNİK ÜNİVERSİTESİ

1 INTRODUCTION

1.1 Literature Review

1.1.1 Antenna Design for Intelligence Transportation Systems

The terms "Intelligence", "Smart", "Sustainable" and "Green" are being used commonly in many fields of our Daily lives such as agriculture, medicine, industry, communication etc. with respect to ever growing needs megacities and metropolis, the amount of environment pollution, road traffic accidents, and security problems are also increased. Intelligence Transportation Systems (ITS) is a research field in which researchers study methods and solutions to overcome mentioned problems of transportation systems in an environment friendly, low cost, and sustainable ways to reach maximum efficiency in transportation systems.

The main aim in ITS is to reduce the work load of human personnel and possible human mistakes during all operation process. Design of high performance electronic stages for wire/wireless communication of ITS systems is an important research topic in fields of Machine to Machine (M2M) and Internet of Things (IOT) [1-2].

With developments in field of ITS, their applications are also expanded. Today many vehicles are actively using Global Position System (GPS), Wireless network communication (Wi-Fi, WiMAX, WiBro) or mobile networks (4G, 4.5G, 5G, LTE), RF or IR waves, alongside of other type of sensor for increasing the safety of passengers and increasing the efficiency of other ITS [3], such as (i) data collection and transfers that would resulted in marked services quality improvement offered to end customers [4-5] (ii) long range communication systems for vehicles [6-8], (iii). Automotive radar applications, where these designs has usage of pre-crash sensing / control firing of restraints, airbags / break boosting, stop & go function of engine, lane change warning and/or aid, blind spot detection, parking aid and back drive

assistance. In most of these applications microwave RF systems are the key elements of mentioned designs [9-15].

With the ever increasing need of technology and complexity of systems and their environments, need of high performance microwave antenna designs is also increased. This encourage microwave engineers to study for novel methods of modelling and prototyping processes to answer the high demand of industry. In this thesis in order to achieve such designs to response the demands of industry, not only novel and high performance antenna design such as, microstrip tapered traveling wave antenna, and multilayered cylindrical dielectric lens antenna have been studied, but also modelling techniques based on artificial intelligence have been employed for design optimization process of computationally efficient antenna designs such as microstrip substrate integrated waveguide antennas and large scale reflect arrays.

1.1.1.1 Traveling Wave Antenna

In recent years with the fast development of the technology, the demands for reconfigurable smart antenna designs capable of dynamically changing their properties, e.g., beam steering, operational frequency and polarization have received a great deal of attention in many applications such as RADAR, transportation and space applications. The advantage of pattern reconfiguration is that it increases the power consumption efficiency at the transceiver stage while it improves transmission and coverage capacity [16-18]. In human detection and scanning applications, the RADAR system requires a narrow beam pattern with fast steering ability where the basic radar functions such as pattern control, scanning, targeting has a critical importance. Although the design procedure of these types of antenna models are relatively complex compared to traditionally designs there have been series of works to achieved this challenging problem, usage of mechanical gears, [19] modification of feeding systems phase, [20] and modifications of surface currents via use of switches [21-31], or by use of substrate integrated waveguide designs [32].

Herein, in order to reduce the complexity and cost of reconfigurable antenna designs, Traveling/ Leaky Wave Antennas (TWAs) design are worked out. TWA

design is based on the traditional microstrip array antennas which was proposed by W. Menzel in 1979 [33]. Thus, this microstrip TWA design has advantages of simple design schematic, low profile, and easy impedance matching. TWAs have been studied as solutions for gain enhancement of simple radiating sources [34-40], sidelobe level reduction [36-39], and radiation pattern reconfiguration [40–49]. By designing a TWA for RADAR systems in [45], an effective continuous scanning has been achieved with a small increase in the feeding signal's frequency, thus it is possible to optimize the range and propagation pattern of the radar array, and steer the pattern of antenna for a scanning in time. Furthermore in [46], [47], substrate integrated waveguide has been used in the design of the TWA in the X –and Ku bands. In [48], beam scanning has been achieved through broadside in dielectric image line environment in the same bands.

In this thesis, a broadband Traveling Wave Antenna (TWA) will be presented as a microstrip design that is capable of a wide range of beam scanning by changing the operation frequency within 8-14 GHz which will be explained in details in the next sections.

1.1.1.2 Microstrip SIW Antenna

The SIW design is a family member of substrate integrated circuits that include other substrate integrated structures such as substrate integrated image guides and substrate integrated non-radiative dielectric guides [49]. SIW components are popular thanks to being easy to design and realized, and have the combined advantages of planar printed circuits and metallic waveguides. Just like microstrip and coplanar transmission lines, SIW components are compact, flexible, and cost efficient. Furthermore, SIW design also have the advantages of conventional metallic waveguides, such as shielding, low-loss, high quality-factor and high-power handling [49]. In this way, the concept of system in Packet (SiP) can be extended to the System on- Substrate (SoS). SoS represents the ideal platform for developing cost-effective, easy-to-fabricate and high performance mm-wave systems.

Recently, especially antenna designs with SIW technology are becoming a trending topic for novel, high performance, low-cost antenna design [52-58]. Antennas designed with SIW technology have excellent performance due to the ability of

suppressing surface wave propagation, wider operation band, decreased end-fire radiation and cross-polarization radiation. Typically, in [52-53], the effect of adding SIW structure to the proposed antenna was presented and gain was measured to be enhanced up to 4 dBi.

In this thesis, design optimization and fabrication of a high performance Microstrip dual-band SIW antenna is studied. The optimization process is achieved via the use of a multi objective meta-heuristic optimization algorithm. Both of antenna design procedure and Optimization algorithm had been explained in details in upcoming sections of the thesis.

1.1.1.3 Multilayered Dielectric Lens Antenna

High gain antennas are one of the vital components in the versatile wireless systems spanning from radio astronomy and radar to satellite communication. One conventional technique for high gain antenna design is the antenna array design. However, this design method has a major disadvantage of transmission loss due to the increase in the number of feeding elements or complexity of feeding network with the result of degradation in the total antenna efficiency in addition to the requirement of precise geometric positioning of radiating elements for low mutual intercoupling. Another design technique of the high gain antennas is to excite the multimode resonance field patterns of a dielectric lens fed by a primary source in the form of single feed or array termed as dielectric resonator antennas (DRA) which are widely used in millimeter wave applications including automotive radar systems [59, 60], satellite transmission components [61] and indoor communication networks [62]. These antenna types have the advantages of wide bandwidth, good radiation stability over the operation frequency band with a high gain. However DRA designs suffer the disadvantages of being bulky with complex geometrical shapes that are either infeasible or impossible to be prototyped via traditional manufacturing methods. Another solution for high gain antenna designs is Dielectric lens antennas. Dielectric lenses are conventionally used in focusing to enhance directivity of the primary radiating source. Similar to the glass lenses frequently used in the optical field [63], dielectric lenses are used in the microwave antenna designs to improve antenna gain characteristics since they are capable of converting incoming quasi-spherical wave into almost plane wave. In literature, there are many different types of microwave lens implementations for the antenna gain improvements [63–66].

Herein, design and realization of a broadband, high performance 3D printed modified Multi-Layered Cylindrical Dielectric Lens Antenna (MLCDLA) are carried out. In the upcoming section the design procedures and its prototyping process via 3D printers had been explained in details.

1.1.1.4 Reflectarray Antenna

Reflectarray antennas (RA) have been of high interest due to the unique advantage of combining the best features of both reflectors and phased array antennas especially in antenna gain that can be achieved without using any complicated feeding network. Microstrip RAs have both electromagnetically and mechanical advantages: From an electromagnetic perspective, they are high gain antennas, low side-lobes, capable of beam steering, and from a mechanical perspective, they have light weight structures, easy to fabricate and manufacture and also robust [67-69].

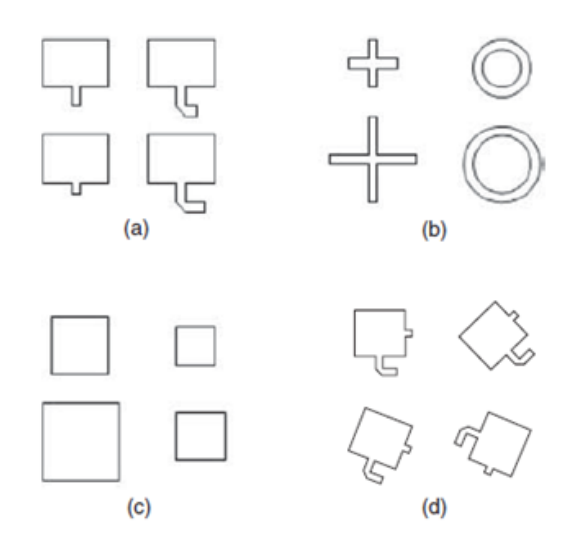


Figure 1.1 Typical RA Unit Elements with Phase Compensation Reflection w.r.t Variable (a) Transmission Line Lengths, (b) Dipoles' and Rings' Sizes, (c) Patch's Size, (d) Elements' Rotations[3]

Microstrip RAs are composed of many isolated patches elements on a substrate (ϵ_r , $\tan \delta$, h) which are various forms such as square, circle, rings (Fig. 1.1) and able to reflect the incident wave independently with a phase compensation proportional to

the distance from phase centre of the feed-horn to form a pencil beam in a specified direction (Θ^0, φ^0) as is well-known from the classical array theory. Thus "Phasing" is a very important process in designing reflectarray. In literature different approaches of compensating the phase of each element have been proposed (Fig. 1.1).

In Fig. 1.1, typical patch forms used in the microstrip RA designs are presented with their phase compensation methods. One of the methods for the reflection phase compensation is to add with a variable stub length in a microstrip patch [70-75]. Another method which is often used is to change the sizes or rotation angle with certain degrees of the unit elements such as rings or dipoles [72-74], and thus the reflection phase characteristics of a RA can be built up [75]. In Fig. 1.2, a traditional planar RA design is presented alongside of its feeding antenna. In Fig. 1.3, a traditional large scale planar RA with variant transmission line patches had been presented.



Figure 1.2 A Traditional RA Design with the Feeding [69]

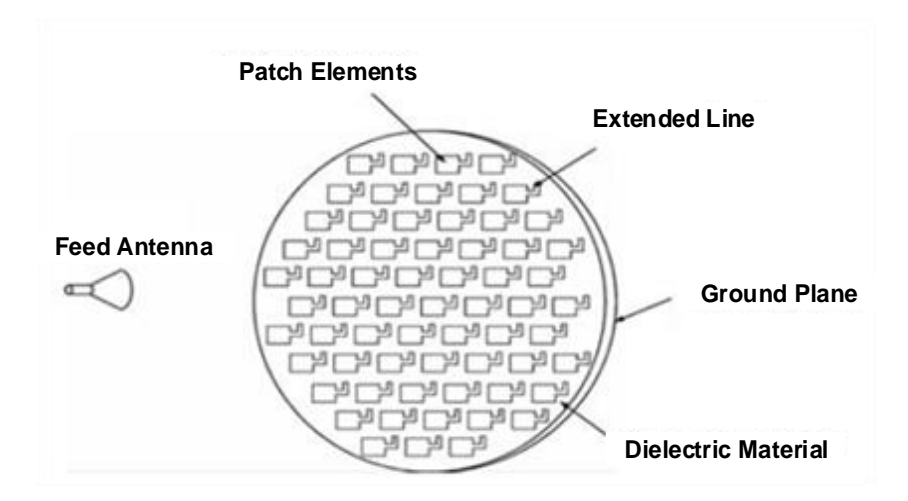


Figure 1.3 A Traditional Large Scale Planar RA with Variable Stub Length Patch Element [69]

Since RA designs are simply hybrid of a reflector antenna and a planar phased array antenna in a compact size and low profile design [76-80], they are mostly preferred in applications such as satellite communication where the designs can be folded and reshaped easier to traditionally designs.

However, microstrip RA designs usually suffer with a narrow bandwidth characteristic caused by intrinsic narrow bandwidth of a microstrip patches and spatial phase delays between the feed and unit cell elements [81]. Some of the methods for enlarging the operation band of microstrip RA designs are: (i) Utilization of dielectric substrates with high thickness, (ii) Having unit element designs with multilayers [82-83]. By using these methods it is possible to increase the bandwidth up to %15.

For design of a MRA, in order to satisfy requirements as the capability to radiate a shaped beam or multi-beams, also to enhance the frequency behavior and bandwidth, novel, complicated patch configurations on multi-layers are needed. Thus, the MRA design problem becomes a massive multi- objective multi-dimensional optimization problem that is not computationally efficient and feasible due to its high mesh size that might take days of simulations even for a few iterations [84]. Therefore first of all for a computationally efficient optimization process, an accurate and rapid model for the reflection characteristic of a unit element is needed to establish as a continuous function within the input domain of the patch geometry

and substrate variables, then it could be convenient to carry this model out adopting a hybrid "global + local" optimization method to find the best solution among all the possible solutions [85-88].

1.1.2 Artifical Intelligence Based Algorithms

In order to achieve high performance the complexity of microwave stages are increased alongside of their simulation durations. Thus, usually the design and optimization process of such designs are computationally inefficient or extremely time consuming. Recently many advance artificial inelegance based methods had been used for (i) creating a surrogate modelling of 3D EM based simulator that has a fast and accurate response, (ii) as an advance search tools to find an optimal solution of multi dimension multi objective optimization problems in fields of microwave engineering. In this thesis, Differential Evolutionary Algorithm (DEA) and Artificial Neural Network had been used for achieving high performance antenna designs via a computationally efficient way.

1.1.3 Meta-Heuristic Optimization

Meta-heuristic algorithm is an advance procedure to form a heuristic that can find an efficient solution to a given problem, especially in case of problems with incomplete or imperfect information. Examples for these methods are: Methods that inspired from the behavior of animal and microorganism, such as particle swarm optimization, artificial immune systems, and insect colonies like Ant or Bees. Most of the mentioned methods have been utilized in design optimization of microwave device and antennas [89-95].

Differential Evolutionary Algorithm (DEA) is a method of multidimensional mathematical optimization which belongs to the class of Evolutionary Algorithm (EA). DEA is originated by Kenneth Price and Rainer M. Storn and first publication of idea of this method was published as a technical report in [96-97].

1.1.4 Artifical Neural Network

A commonly used novel method for creating an accurate and fast numerical models of microwave devices is Artificial Neural Networks (ANN) which is a simplified mathematical model of the biological neural network. Particularly Multi - Layer Perceptron type of Neural Network (MLPNN) has found a lot of microwave modelling and optimization applications [98-110]. A MLP NN is composed of a collection of interconnected neurons taken place in the input, output and hidden layers where neurons have activation functions to be used in the mapping process between the input and output domains. A MLP NN architecture matrix consists of weighting coefficients belonging to the interconnections and the bias values, which are determined by an optimization process called the training process using the simulated or measured data sets as the target data. Then validation of the ANN model is made by the prediction process via the defined test criteria and data. Thus the ANN is ready for the regression process consisting of accurate and rapid prediction of the outputs corresponding to any given input vector within the input domain. In the other words, the outputs are obtained numerically as continuous functions of the input variables expressing nonlinear mapping between the input and output domains. In the applications of modelling of microwave devices, these inputs may be geometry and substrate parameters of a microstrip patch antenna or DC bias conditions and operation frequency of a microwave transistor, etc, where the outputs may be gain and resonance frequency, the Scattering parameters, respectively, of the related devices [101-108].

1.1.5 3D Printing Technology

Furthermore in order to have a fast, reliable low cost and accurate prototyping process, 3D printing technology had been used for manufacturing of some of the proposed antenna designs.

Components with three-dimensional (3D) geometrical structure have gained significant interest in the recent years due to the final innovations in 3D printing technology. Nowadays, 3D printers are extensively used in many applications ranging from medical, industrial art, jewellery, automotive industry to electronic circuits. Due to the layer by layer construction ability, 3D printers have the advantage of prototyping of complex designs that are extremely difficult and expensive to prototype with the conventional fabrication methods. Especially in the field of microwave circuit designs, 3D printers have received great attention due to

the precise, fast, and low cost manufacturing capabilities for the prototyping of versatile RF circuits and components.

Although there are many types of 3D printing process such as Stereolithography (SLA), Digital Light Processing (DLP), Laminated object manufacturing (LOM), Fused Deposition Modelling (FDM), Selective Laser Sintering (SLS), Selective Laser Melting (SLM) and Digital Beam Melting (EBM), FDM and Direct Metal Laser Sintering (DMLS) have been used extensively in prototyping of microwave component. In [111-113], applications of DMLS and printing for manufacturing of waveguides, waveguide-based passive microwave components, antennas, and antenna arrays were studied. In [114, 115] application of metallic printers for prototyping of horn antenna designs was studied. Although metallic printing is an effective prototyping method, FDM printing has also been used for 3D printing of microwave stages, such as reflectarray antennas [116, 117], flexible antennas [118,119], multi-layered dielectric loaded antenna [120], quasi-Yagi antenna [121], microstrip patch antenna [122], X-band horn antennas [123], realization of dielectric sheets for gain improvement of ultra-wideband horn antennas [124].

1.2 Objective of the Thesis

In this thesis, it is aimed to propose different antenna designs and novel design methodologies in order to answer the ever increasing need of wireless technology for applications of Intelligence Transportation Systems. Each of the studied designs is aimed to meeting to a different need of communication such as automotive radar, Satellite communications etc.

1.3 Hypothesis

In order to achieve the goal of the thesis, 3D EM simulation tools have been used for design procedure of antennas. The studied antennas in this thesis are multi-objective multi dimension optimization problems that requires high performance search tools. Differential Evolutionary Algorithm (DEA) which is a Meta-Heuristic base optimization algorithm and that have shown great potential in many microwave applications including design optimization of antennas. However due to their limitations of computation efficiency, these tools are not efficient solutions for

large scale multi objective. Thus, in order to solve this problem, Artificial Neural Network based surrogate models of 3D EM simulators have been generated to be used as an accurate reliable and fast solution for design optimization process. Furthermore, for justification of the proposed antenna designs and their designs methodologies, a low cost, fast and accurate prototyping process have been used via the usage of 3D printing technology. The measured and simulated results of the designs have been compared with performance of counterpart designs in literature to clearly demonstrate the achievement of the proposed methodologies.

2.1 Microstrip Tapered Traveling Wave Antenna for Wide Range of Beam Scanning in X- and Ku- Bands

As it mentioned before, with the fast development of the technology, the demands for reconfigurable smart antenna designs capable of dynamically changing their properties, e.g., beam steering, operational frequency and polarization have received a great deal of attention in many applications such as RADAR, transportation and space applications. In this chapter, in order to reduce the complexity and cost of reconfigurable antenna designs, Traveling/ Leaky Wave Antennas (TWAs) design are worked out. TWA design is based on the traditional microstrip array antennas which was proposed by W. Menzel in 1979 [33]. Thus, this microstrip TWA design has advantages of simple design schematic, low profile, and easy impedance matching. TWAs have been studied as solutions for gain enhancement of simple radiating sources [34-35], side-lobe level reduction [36-39], and radiation pattern reconfiguration [40-44]. By designing a TWA for RADAR systems in [45], an effective continuous scanning has been achieved with a small increase in the feeding signal's frequency, thus it is possible to optimize the range and propagation pattern of the radar array, and steer the pattern of antenna for a scanning in time. Furthermore in [46], [47], substrate integrated substrate have been used in the design of the TWA in the X -and Ku bands. In [48], beam scanning has been achieved through broadside in dielectric image line environment in the same bands. Herein, a TWA design is achieved as a simple microstrip tapered travelling wave antenna that is capable of a wide range of beam scanning by changing the operation frequency within 8-14 GHz. Furthermore with the usage of the proposed patch load (PLTWA) instead of traditionally resistive load, efficiency

and gain characteristics are increased along the operation band. Dimensions of the proposed TWA is 130×30 mm. The fabricated TWA operates over 8-14GHz with a fractional bandwidth, and it exhibits a peak gain of 9.5 dBi at 11 GHz. The measured gain of the proposed antenna is around 9-12 dB and the main beam direction is steerable with the range of 80° (-65° to 15°). Thus, with the proposed patch loaded TWA design it is achieved to increases the maximum gain almost 3 dB and the total efficiency up to 90% compared to the traditional resistive load over the operation band of 8-14 with a steerable beam range of 80° (-65° to 15°). Besides, scan range, peak gain and dimensions of the proposed design will be compared with the counterpart design in section of the experimental results. The detailed antenna structure and design principles are briefly explained in section 2.1.1. The experimental verification of the proposed TWA is provided in Section 2.1.2 alongside of the comparison table for the design operates in similar operation band. Finally, the work ends with a brief conclusion in Section 2.1.3.

2.1.1 Design and Simulation of Microstrip Tapered TWA

TWA designs use a travelling wave on a guiding structure as the main radiating mechanism. TWA designs usually consist of open-ended wires where the current must go to zero. The surface current on TWA designs can simply considered as a superposition of electromagnetic waves traveling in the opposite directions. A TWA can be simply designed by a single wire transmission line alongside of a matched load termination (Fig. 2.1(a)). Typically, the length of the transmission line is several wavelengths [125].

TWA are usually consist of periodical structures. The direction of the antenna's main beam is highly dependent on the geometrical design parameters. The most commonly geometries used on design of microstrip patch antennas are as follows: chain, trapezoidal, comb, saw geometries. In Fig. 2.1(b) some traveling wave antenna had been given.

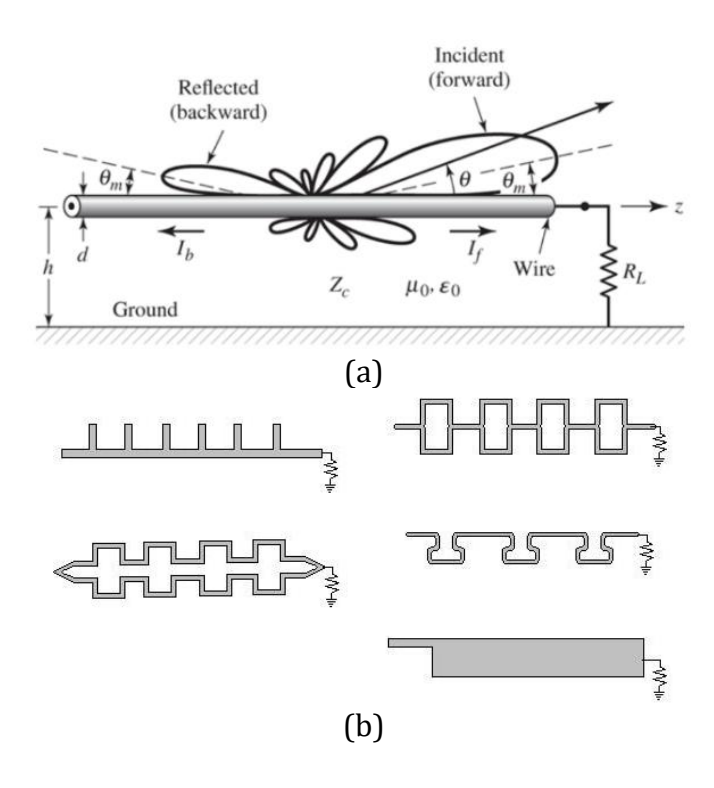


Figure 2.1 (a) An Example for a TWA Design (Beverage antenna) [124] (b) Basic Shapes of the Travelling Wave Antennas [45]

Main beam direction of the radiation is determined by the phase velocity of travelling waves, thus by taking advantage of dispersive effects of feeding signals frequency on waveguides it is possible to obtain a design with steerable beam. In this section, design and simulation results of a traditional Traveling Wave Antenna and the proposed patch loaded design are investigated. As it can be seen from Fig. 2.2(b), the traditional TWA design consists of a resistive load which would decreases the total efficient of antenna design.

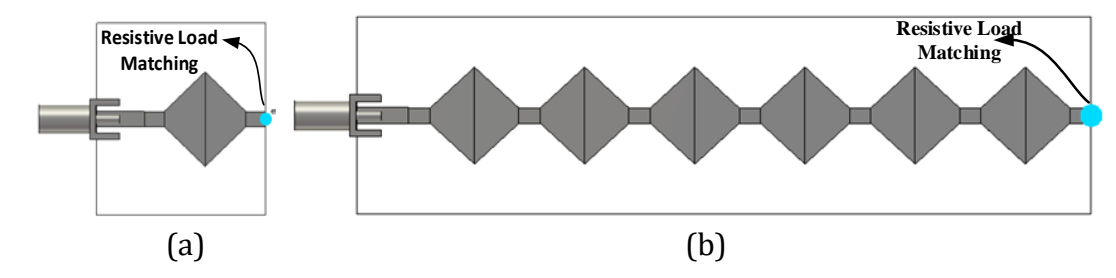


Figure 2.2 (a) Unit Cell Design (b) Traditionally Resistive Loaded Travelling Wave Antenna Design

Herein it is aimed at increasing efficiency of the TWA design along the operation band by using a patch antenna load instead of a resistive load and a tapered-shaped line given in Figs. 2.2-2.3. Operation frequency of broadside radiation of the unit cell is located around 8 GHz to 14GHz in Fig. 2.4(a). Optimization and simulation processes are carried out using 3-D Microwave Simulation software CST. The following design parameters are the most crucial factors that should be taken into the consideration during the design process (Fig. 2.3):

- In order to increase / decrease the gain of design the number of elements can be increased / decreased;
- To increase the input impedance of design, the number of elements can be increased;
- By increasing substrate height, patch widths or decreasing the materials permittivity, the band width can be increased;
- To increase beam scanning range the length of the microstrip line can be increased, otherwise vice versa.

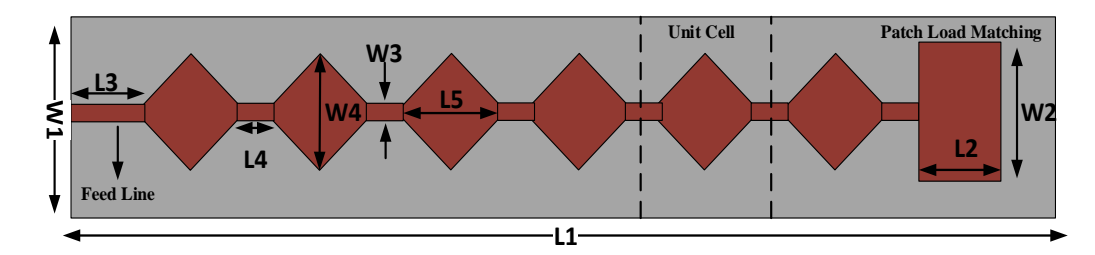


Figure 2.3 The Proposed PLTWA

The proposed Patch Loaded Traveling Wave Antenna (PLTWA) and its optimally selected design parameters of are given respectively, in Fig. 2.3 and Table 2.1. The values given in Table 2.1 are obtained via a design optimization process by using differential evolutionary optimization algorithm [125]. In Eq. 2.1, the cost function for design optimization of PLTWA had been given.

$$Cost(L_i, W_i, fr) = min\{S_{11}\} + max\{Gain\}$$
(2.1)

where; $L_i:L_{1-5}$, $W_i=W_{1-4}$, f_r : the cost function is valid over the operation frequency only.

The PLTWA model is designed on a Rogers RT/Duroid 5880, ε_r = 2.2, $\tan\delta$ = 0.0009, height h = 0.79 mm with a metallic ground at the bottom alongside of a 50 Ω matched SMA-connector on the feed line for the measurements.

The simulated S_{11} , Maximum Gain, and total efficiency over the frequency are presented in Fig. 2.4. As it can be seen from Fig. 2.4, termination the antenna by a rectangular patch load increases the maximum gain almost 3 dB over the operation band and the total efficiency of the system is increased up to 90% compared to the traditionally resistive load design at the expanse of a small distortion on S_{11} characteristics.

Table 2.1 Parameter List of PLTWA Design in mm

W1	30	L1	130
W2	15.68	L2	10.12
W3	2.35	L3	11.38
W4	14.8	L4	3.3
h Substrate	0.79	L5	13.67

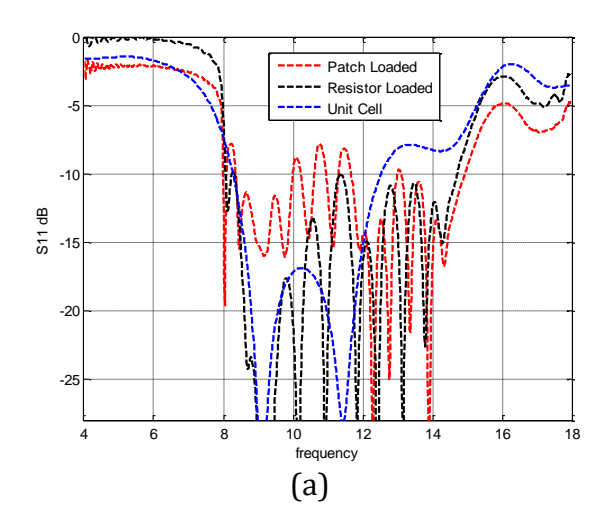


Figure 2.4 Simulated (a) Return Loss (b) Maximum Gain (c) Efficiency of TWA Design

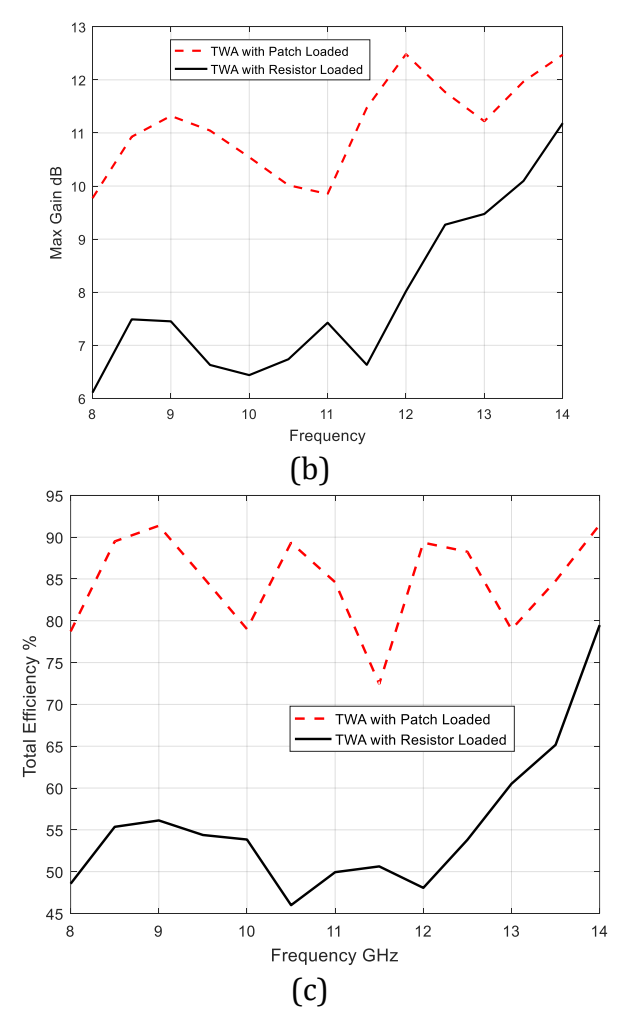


Figure 2.5 Simulated (a) Return Loss (b) Maximum Gain (c) Efficiency of TWA Design (continued)

Fig. 2.5 depicts the radiation characteristics of the proposed PLTWA design with respect to the variation of frequency. Also in Table 2.2, a detailed comparison of the traditionally resistive loaded TWA and proposed PLTWA is presented. As it can be seen from the table, the proposed patch loaded TWA design it is possible to enhance the radiation characteristics of the antenna such as side-lobe level, beam width or gain value. With the increase in the efficiency of the PLTWA, the gain characteristics of the antenna has been enhanced up to 4.5 dB over the operation band. The efficiency of the antenna has been calculated from the 3D EM simulation results of CST by using Eq. 2.2 [36]. In the next section the experimental results of the proposed PLTWA had been studied.

$$e_{cd} = \frac{R_r}{R_L + R_r} \tag{2.2}$$

Where; e_{cd} is radiation efficiency, R_r = radiation resistance, R_L = resistance representing the combination of the conduction-dielectric losses of the antenna design [126].

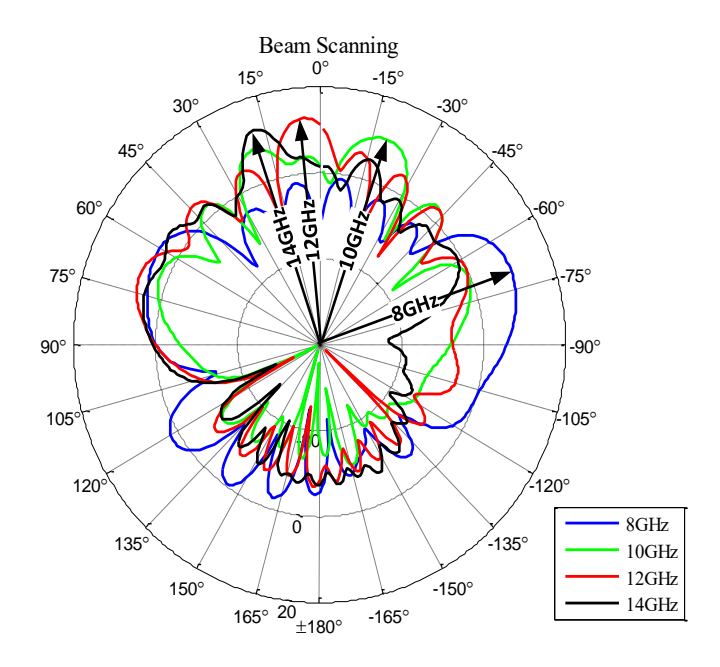


Figure 2.6 Simulated Radiation Pattern of PLTWA for Variant Frequencies

Table 2.2 Simulated Performance Comparisons of Resistive Loaded TWA and PLTWA

f (GHz)	S ₁₁ (dB)	Realized Gain (dB)	Enhanced (dB)	Main Lobe direction (Angle)	3dB (Angle)	Side lobe level (dB)	Efficiency %
8	<-10/ <-8	6.18 /9.77	+3.59	68 /70	30.8 /28.6	6.8 /4.8	47 /78
9	<-10/ <-8	7.45 /11.4	+3.95	40 /39	17.6 /14.2	6.3 /5.5	56 /92
10	<-10/ <-8	6.44 /10.6	+4.46	25 /19	23.2 /15.1	5.4 /2.4	54 /80

Table 2.3 Simulated Performance Comparisons of Resistive Loaded TWA and PLTWA (continued)

12	<-10/ <-8	8.01 /12.5	+4.49	2 /4	15.7 /6.2	5.2 /6.2	47 /89
13	<-10/ <-8	9.5 /11.2	+1.7	9 /9	11.8 /10	6.3 /6.8	60 /78
14	<-10/ <-8	11.8 /12.5	+0.7	16 /20	10.1 /9	5.2 /7.7	80 /93

2.1.2 Experimental Results

In this section, the optimized antenna is fabricated using LPKF ProtoMat S series [127]. The fabricated prototype is shown in Figure 2.6, along with the simulated and measured S_{11} and gain characteristics. For measurement of the PLTWA a Network Analyzer with a measurement bandwidth of 9 KHz -13.5GHz, and reference antenna in [128] are used.



Figure 2.6 Fabricated PLTWA

The measured return loss characteristic, maximum gain- total efficiency over the operation band and the measured radiation pattern for varying frequencies are presented in Figs. 2.7-2.9 and Table 2.3. It can be seen that the measured and simulated results are in good agreement where the slight variation occurs due to fabrication tolerances.

Table 2.3 Sample Table Measured Performance of PLTWA

fr	S ₁₁ (dB)	Main Lobe Angle	Gain (dB)
(GHz)			
8	-10	-65 ⁰	9.2
9	-10	-400	10.3
10	-20	-200	10.1
11	-12	00	9.5
12	-18	50	12
13	-8	10^{0}	10.7
14	-13	-15 ⁰	11.1

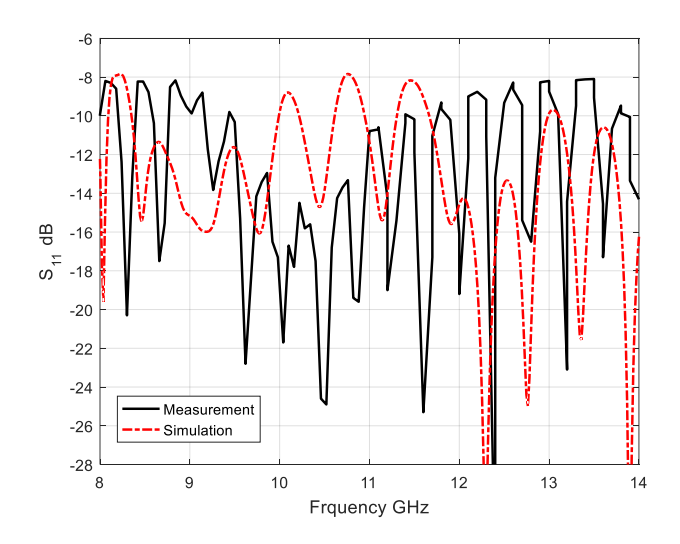


Figure 2.7 Simulated and Measured S₁₁ of PLTWA

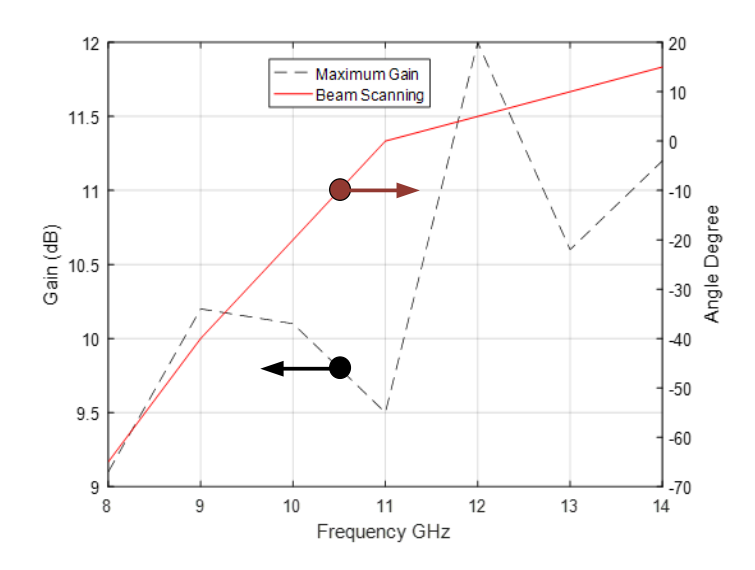


Figure 2.8 Measured Gain and Beam Scanning with Frequency

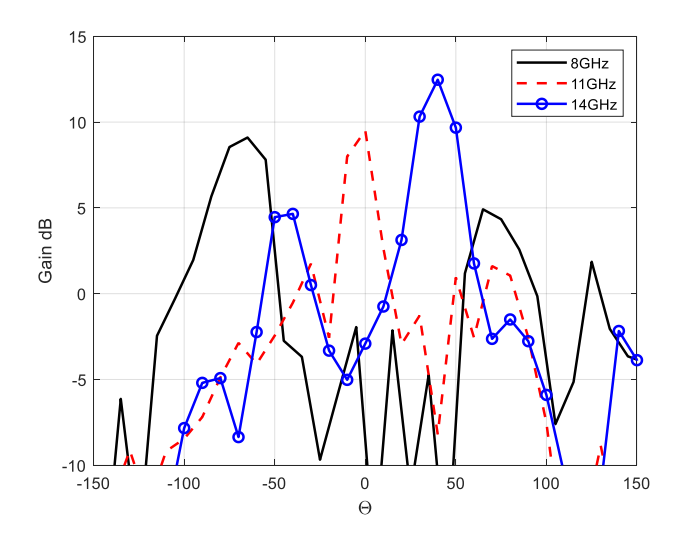


Figure 2.9 Measured Radiation Pattern for Variant Frequencies

The variation of the main lobe direction of the antenna is shown in Fig. 2.9. The direction of the main lobe is scanned from -65° at 8 GHz to 15° at 14 GHz.

Finally, the performance of the proposed PLTWA is compared with counterpart designs that are reported in literature in Table 2.4. In [30], design of a resistive load microstrip traveling wave antenna for X band applications at 9-10 GHz band had been studied. The design has a peak gain value of 13 dB with scanning range of 0 to 27 degree. In [31] authors achieved to design a miniaturized leaky-wave antenna by

using quarter-mode SIW operating in operation band of 12.5-15.4 GHz with a scanning range of 0-28 degree. In [32], the authors proposed a continuous beam scanning by applying substrate integrated waveguide to the leaky-wave antenna design. In [33] design of a broadband (%33.2) leaky wave antenna with dielectric image line had been proposed for Ku-band applications within the range of 11.3–15.8 GHz with scanning range of -60 to 38 degree. The proposed design requires a planar structure and obtains less dispersive beam scanning compared with a composite right/left-handed (CRLH) leaky-wave antenna design. From this table, one can easily observe that both the gain and the scan range of the proposed PLTWA are better than the counterpart works.

Table 2.4 Comparison of PLTWA with Counterpart Designs in Literature

Design	f (GHz)	Scan Angle Range	Peak Gain (dB)	Length
Here	8-14	-65º to 15º	12	130mm
[45]	9-10	0º to 27º	13	171mm
[46]	12.5-15.4	0° to 28°	13.17	316mm
[47]	11.3-15.8	-60° to 38°	15	170mm
[48]	9-14	-40° to 35°	12	140mm

2.1.3 Discussion on Performance of Proposed TWA

Herein, design of a microstrip patch loaded traveling wave antenna (PLTWA) is presented for the aim of: increase the total efficiency and gain performance of traditionally TWA designs. The proposed PLTWA design has a frequency depended pattern steering in operation band of 8-14 GHz with the dimensions of $30 \times 130 \text{ mm}^2$. The fabricated PLTWA operates over 8-14GHz with a fractional bandwidth, and it exhibits a peak gain of 9.5 dBi and at 11 GHz. The measured gain of the proposed antenna is around 9-12 dB and the main beam direction is steerable with the range

of ($-65^{\circ}\sim15^{\circ}$). The comparison of the proposed PLTWA with counterpart works shows that the design have a better performance. The proposed PLTWA is simple to design and fabricate and can be used in basic radar functions such as search, detection, tracking, guidance, and electron beam control applications. Also, the proposed PLTWA design can be easily adapted and realize in the higher mm-wave frequency band with adequate performance.

SUBSTRATE INTEGRATED WAVEGUIDE ANTENNA

3.1 Design Optimization of a Dual- Band Microstrip SIW antenna Using Differential Evolutionary Algorithm for X- and K- Band Radar Applications

In this thesis, SIW technology is applied to design a microstrip dual-band antenna for X and K band radar applications. An antenna model given in Fig. 3.1 [53] is considered as an efficient antenna model for the aimed operation frequencies. Roger 4350 (ϵ_r =3.48) with 1.52mm height is used as a low-cost substrate of the SIW.

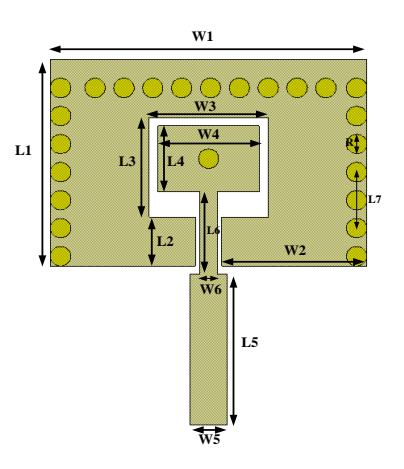


Figure 3.1 Parametric Layout of SIW Antenna

The design optimization process of the proposed SIW antenna model is achieved via the use of Differential Evolutionary Algorithm (DEA) in 3D CST Microwave studio environment. For this purpose, the microstrip SIW antenna design problem is converted to an optimization problem by defining optimization variables and objectives based on the antenna performance criteria such as gain and return loss characteristics. Then, in order to prove the success of the design optimization of SIW antenna, a prototype is built with the optimal design parameters obtained from the

DEA process and measured its performance. The measurements verify that the proposed microstrip SIW antenna model is a sufficient solution for X and K band radar applications and the DEA algorithm is an efficient algorithm for design optimization of microstrip SIW antennas.

3.1.1 Desgin Optimization of Dual-Band SIW Antenna Using DEA

Roger 4350 (ϵ_r =3.48) with 1.52mm height is used as substrate of the SIW antenna and the optimization variables are dimensions of the rectangular microstrip patch, feedline size, the total number of metallized via's and their gaps as given with their limitations in Table 3.1.

Table 3.1 Constraints of the Variables in (mm)

Parameter	Parameter Constraint		Constraint
W1	10~20	L1	5~15
W2	1~10	L2	1~10
		L3	1~10
W4	1~10	L6	1~10

The geometrical design parameters can be increased or decreased based on the request of designer, furthermore design parameters such as distance of via's, diameter of via's or other parameters such as dielectric constant or height of substrate can be added. But it should be noted that with the increase in number of optimization variables the search space would become more complex and requires more function evaluations which would drastically decreases the computationally efficiency of the design process. Also it should be taken into consideration that decreasing number of variables might prevent the algorithm to find the optimal solutions in the limited search space.

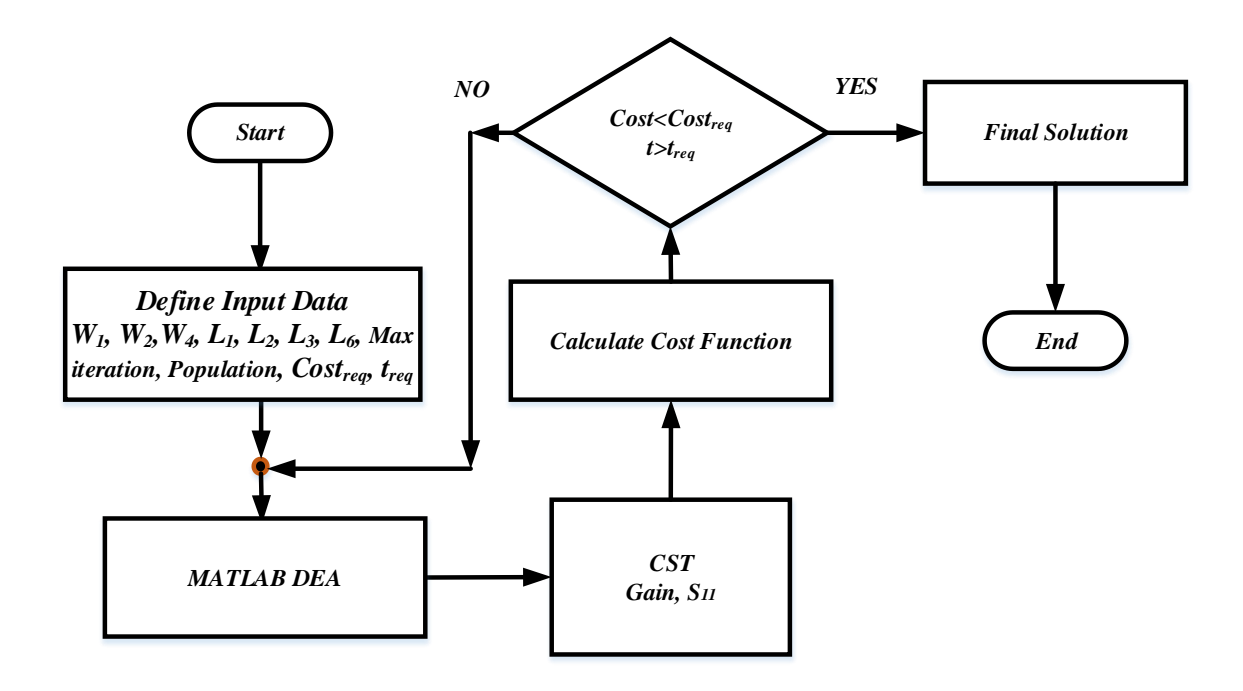


Figure 3.2 Flow Chart of the SIW Antenna Design Optimization

The flow chart of the optimization process is given in Figure 3.2. According to this flow chart, it can be observed the DEA working in MATLAB environment send the optimization parameter values to CST suit environment to start a 3D electromagnetic simulation process. Then the simulation results in CST environment are sent to MATLAB environment in order to evaluate the cost function of the optimization process:

$$Cost_{i} = \frac{C_{1}}{Directivity_{i}} + \frac{C_{2}}{\left|S_{11_{i}}\right|}$$
(3.1)

where, C is weighted constrained determined by user (Here in C_1 =0.9, C_2 = 0.3 which is determined with trial and error method), both S_{11} and directivity are only taken into account at the requested operation frequencies, 12 and 24 GHz; i is the index of the current member of DEA population. The performance results are obtained after 10 independent runs of the optimization process and the specification criteria of the objective function are:

$$S_{11}dB < -10$$
 $f = 12GHz \text{ and } 24GHz$ (3.2)

Max(Directivity)
$$f = 12GHz \text{ and } 24GHz$$
 (3.3)

In Tables 3.2-3.3, the performance results of DEA algorithm for 10 different runs are presented. In Table 3.2, the best, worst and mean performance results of DEA for these 10 runs are given. As it can be observed, when the population size is taken as 20, the optimization process cannot converge to the required cost value and are trapped in a local minima in the search domain. However when the population size is increased the overall performance of the DEA is also increased. However it should be noted that although the increased number of population might also increases the performance it also would decrease the computationally efficiency of the whole process. This can be observed from Tables 3.2 and 3.3, where the minimal cost value obtained from run with 30 population size is reached to the value of 0.307 the run with 50 population size has achieved 0.278. However, even though the mean performance result of 50 population run is much better than the run with 30 population, the required function evaluation for 50 population is much higher than 30 populated run which will drastically decreases the computational efficiency of optimization process.

Table 3.2 Performance Results of DEA*

2 1	Cost					
Population	Maximum	Minimum	Mean			
20	7.54	2.54	3.88			
30	2.26	0.307	0.916			
50	1.34	0.278	0.613			

^{*}Mean results obtained from 10 different runs at 20 iteration.

Table 3.3 Number of Function Evaluations of DEA*

Population	Iteration				
	5	10	15	20	
20	107	198	289	380	
30	161	297	433	570	
50	268	495	722	950	

^{*} Mean Results obtained from 10 different runs

The parameters given in Table 3.4 are obtained via DEA with 50 population size after a 20 iteration where the minimal cost was found as 0.278 with respect to the limitations given in Table 3.1 and Eq. 3.1.

Table 3.4 Optimal Parameter List in (mm)

W1	15.4	L1	10.7
W2	7	L2	2.5
W3	5.75	L3	5.1
W4	4.95	L4	3.4
W5	2xW6	L5	7.8
W6	0.85	L6	4.2
R	0.8	L7	3.35

The simulated and measured results of the prototyped SIW antenna design (Fig. 3.3) are presented in Figs. 3.4-3.6. The measurement results are obtained using the measurement setup given [129]. The simulated radiation pattern of the optimally

designed SIW antenna are given in Fig. 3.4 where the designed antenna achieves a simulated gain level of 7 and 7.13 dBi at 12 and 24 GHz respectively.

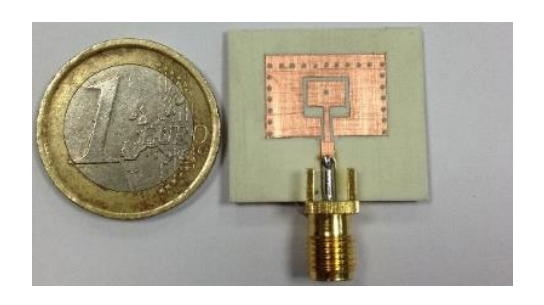


Figure 3.3 Fabricated Antenna

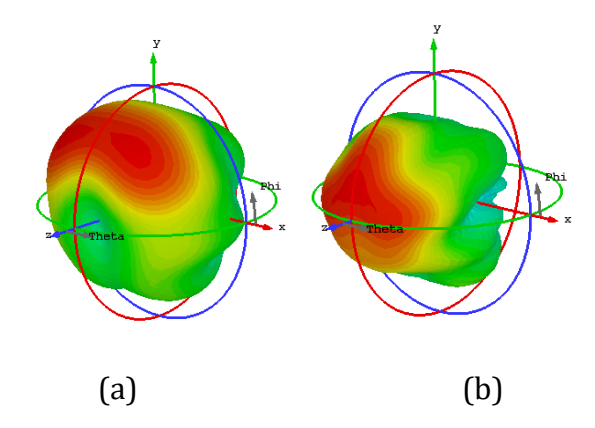


Figure 3.4 Simulated Gain Patterns (a) 12GHz, (b) 24 GHz

For further investigation of the effect of SIW structure on the performance results of antenna designs two additionally simulation cases had been added. (i) an antenna design similar in Fig. 3.1 which does not have any SIW structure with the same geometrical design parameters in Table 3.4 (NO SIW design), (ii) the same No SIW antenna design that is optimized via the DEA (NO SIW OPT). In Fig. 3.5, the simulated performance of antenna design with and without SIW structure had been presented alongside of both simulated and measured performance of the optimally design SIW antenna. Here it should be noted that optimized antenna not only is have resonance frequency in 12 and 24 GHz but also is resonated in middle frequencies. This can be prevented by simply adding these frequencies to the cost function or it is also possible to make the antenna has better performance measures in these frequencies by adding them to the cost function. However in this work simply only performance measures at 12 and 24 GHz are provided to the cost function and optimization process for design optimization of a dual band antenna.

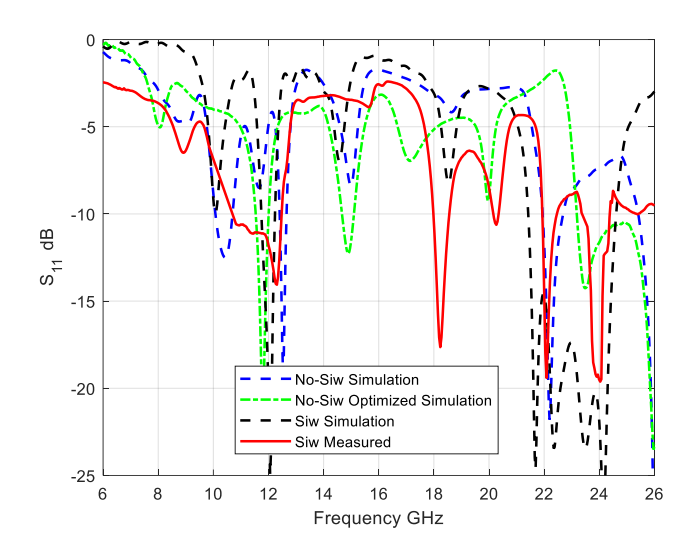


Figure 3.5 Simulated and Measured Return Losses

In Table 3.5 and Fig. 3.6, the simulated and measured gain performance results of the antenna designs are presented. As it can be seen, the best gain performance results obtained from the design without SIW structure, even though an optimization process is applied, is around 6 dB for the selected operation frequencies while after the application of SIW design the gain is increased almost 2 dB. Furthermore, for extending the performance enhancement of SIW structure a comparison analysis with recently published works with SIW designs in literature [130-135] is presented in Table 3.6. As it can be seen from Table 3.6, the proposed design optimization process has achieved an antenna model that not only have better or similar performance results (Gain and S₁₁), but also have realized this performance measure with smaller size compared to counterpart designs even though one of its operation band is at 12 GHz.

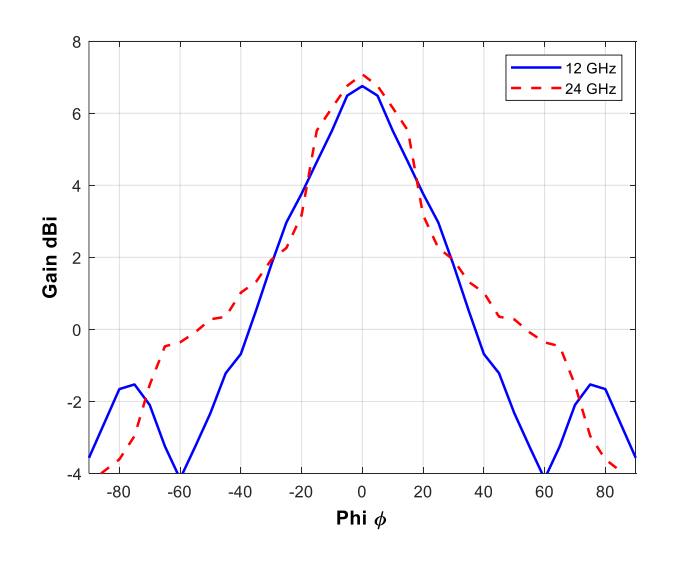


Figure 3.6 Measured Far Field Gain

Table 3.5 Comparison of the Realized Gains

		Realized	Gain (dB)	Di di i (
Model		12GHz	24GHz	Die Size in (mm)	
SIW Measured		6.7	7	25.5x22.5	
	SIW DEA	7.01	7.13	25.38x22.45	
Simulated	No SIW	4.8	5.8	25.38x22.45	
	No SIW DEA	5.1	6.2	23.85x22.45	

Table 3.6 Comparison of Antenna with Literature

Models	f (GHz)	S ₁₁ (dB)	Realized Gain dB	Substrate	Die Size (mm)
Here	12 / 24	-10 / -19	6.7 / 7	Roger 4350	25.5x22.5
[54]	10	-25	9.8		30x30
[130]	15	-15	7.5		30x30
[131]	25	-20		Arlon 25N	15x27
[132]	10 / 12	-30 /-30	8/9	Taconic TLY	40x56
[133]	18.2-23.8	<-15	9.5	Droid 5880	20x25
[134]	25.8- 31.5	<-15	>6	RT/Duroid 5880	
[135]	8-15	<-17	>6	Arlon IsoClad 917	55 × 46.8

3.1.2 Discussion on Performance of Proposed SIW Antenna Design

In this study case, a high performance, miniature, novel antenna is designed and fabricated on a low-cost substrate for X and K band radar applications. For this purpose, design optimization and fabrication of a high performance microstrip dual band antenna using Substrate Integrated Waveguide technology is worked out. Thus firstly, an efficient design optimization of a microstrip SIW antenna has been carried out on a low-cost substrate Roger 4350 with a possible simple geometry as a multi-objective, multi-dimensional optimization problem using the Differential Evolutionary Algorithm (DEA) within 3-D CST Microwave studio environment. At the same time, effects of the SIW structures are investigated on the radiation and return loss characteristics of the antenna design by simulation in different cases

and optimized using DEA. In simulated results, the optimized antenna with SIW structure achieves the simulated gain level of 7 and 7.13 dB at 12 and 24 GHz respectively, while other two cases of antenna design without SIW design can only achieves 6 dB at most. In the second step, for justification of the proposed design method, the optimally designed dual band SIW antenna has been prototyped. Finally it has been reached a conclusion that the competitive performance has been achieved with this miniature, simple microstrip SIW antenna design as compared with the counterpart designs in the literature.

MULTILAYER DIELECTRIC LENS ANTENNA

4.1 A Novel Design of High Performance Multilayered Cylindrical Dielectric Lens Antenna Using 3D Printing Technology

In this study case, design and realization of high performance, low-cost X-band Multi-Layered Cylindrical Dielectric Lens Antenna (MLCDLA) is presented using 3D printing technology. Firstly, MLCDLA is designed and simulated in the complete 3D CST Microwave Studio (MWS) within the X- band as consisting of six layers and being fed through a conventional rectangular waveguide (WR90). These layers are in the form of cylindrical discs having different radii, thicknesses and made of a cheap polylactic acid material. These layers have also varying dielectric constant from 1.2 to 2.7 that are compatible for Fused Deposition Modelling (FDM) based 3Dprinting process. Secondly, a prototype of MLCDLA is produced by using a FDM based 3D-printer. 3-D printed dielectric lens antenna is measured and a good return loss of almost more than 10 dB within the X-band with a high gain of 16-18 dBi are achieved as compared with the counterpart alternative designs. Thus it can be concluded that the proposed novel design and prototyping method not only achieves the high radiation performance characteristics along X-band but also is a fast, low cost and effective method for prototyping dielectric lens structures for the microwave applications.

4.1.1 Design of Multilayered Cylindrical Dielectric Lens

In this section, the design of the proposed multi-layered cylindrical dielectric lens is presented. The proposed antenna design is based on six-layered lens plates fed through a rectangular waveguide. The geometric parameters of each layer are indicated in Fig. 4.1. The technological advance of prototyping abilities of 3D

printers facilitates to use versatile base materials with different dielectric constants to be manufactured by only changing the infill rate of deposited material (the volume fraction of the thermoplastic to the total volume) [122], [136]. Thus, in the proposed antenna design, not only each layer of the lens structure has different height and radius but also dielectric constant values are taken as a design variable for the dielectric lens design. In [122] Eq. 4.1 is presented as a simple expression that calculates the dielectric constant value of a material with respect to the infill rate of the material, based on measured results given in [136], where the variation of dielectric constant with respect to the infill rate (defined in percent within the limits of %15-%100) of material, x has been expressed [122]. By using this equation it is possible to design layers with a variable dielectric constant from 1.2 to 2.7:

$$\varepsilon_{\rm r} = -1.3 \times 10^{-6} \,{\rm x}^3 + 0.0374 \times + \frac{6.42}{\rm x} + 0.217$$
 (4.1)

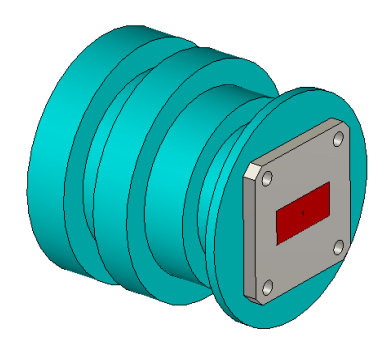


Figure 4.1 Schematic and Geometrical Structure of the Proposed MLCDLA

The flat discs of dielectric lenses are fabricated with a cheap polylactic acid material of dielectric properties varying from 1.2 to 2.7 by a compatible FDM based 3D-printing process subject to Eq. (4.1). The proposed MLCDLA model shown in Fig. 4.1 consisting of six layers of cylindrical discs with variable layer height, layer radius, and layer dielectric constants from 1.2 to 2.7. All of these 18 variables indicated in Table 4.1 are determined via trial and error alongside of using Trust Region Framework (TRF) optimization method embedded in CST provided with the goals of: (i) S11 characteristic of less than -11 dB, (ii) Maximum gain characteristic of more than 16 dBi, over the operation band of 8-12 GHz. Then, finally the determined optimal dielectric constant values in table 4.1 are realized from the reverse of eq. 4.1 adjusting the infill rate of the material to obtain the requested dielectric

constant. The computed results of S_{11} and gain parametric analysis are given for seven different cases in Table 4.2 in Fig. 4.2 and Fig. 4.3, respectively. Furthermore the radiation patterns and E-field distribution of Case 1 at 8GHz, 10 GHz, and 12 GHz are presented in Figs. 4.4-4.5.

Table 4.1 Parameter Values of the Fabricated Lens Case 1

Eps1	1.2	H1*	3	R1*	33.4
Eps2	1.87	H2*	12.6	R2*	20.8
Eps3	2.15	Н3*	13	R3*	27.2
Eps4	2.27	H4*	11.4	R4*	34.8
Eps5	1.9	H5*	10	R5*	26.8
Eps6	2.5	Н6*	12.6	R6*	35

^{*} in (mm)

 Table 4.2 Parameter Values for Parametric Analysis

	Eps1	Eps2	Eps3	Eps4	Eps5	Eps6		
			Same wi	th Case 1				
Case 2	H1*	H2*	Н3*	H4*	Н5*	Н6*		
	10							
	R1*	R2*	R3*	R4*	R5*	R6*		
	Same with Case 1							
Case 3	Eps1	Eps2	Eps3	Eps4	Eps5	Eps6		
	2.5							
	H1*	H2*	Н3*	H4*	H5*	Н6*		

Table 4.2 Parameter Values for Parametric Analysis (continued)

	Same with Case 1									
Case 3	R1*	R2*	R3*	R4*	R5*	R6*				
	Same with Case 1									
	Eps1	Eps2	Eps3	Eps4	Eps5	Eps6				
		,	Same wi	th Case 1						
C 4	H1*	H2*	Н3*	H4*	H5*	Н6*				
Case 4		Same with Case 1								
	R1*	R2*	R3*	R4*	R5*	R6*				
	35									
	Eps1	Eps2	Eps3	Eps4	Eps5	Eps6				
	1	1.25	1.5	1.75	2	2.5				
C	H1*	H2*	Н3*	H4*	H5*	Н6*				
Case 5	10									
	R1*	R2*	R3*	R4*	R5*	R6*				
	35									
	Eps1	Eps2	Eps3	Eps4	Eps5	Eps6				
		,	Same wi	th Case 1						
Case 6	H1*	H2*	Н3*	H4*	H5*	H6*				
			Same wi	th Case 1						
	R1*	R2*	R3*	R4*	R5*	R6*				

 Table 4.2 Parameter Values for Parametric Analysis (continued)

	35	32	29	26	23	20			
	Eps1	Eps2	Eps3	Eps4	Eps5	Eps6			
	2.5	2.5 2		1.5	1.25	1			
Case 7	H1*	H2*	Н3*	H4*	H5*	Н6*			
	10								
	R1*	R2*	R3*	R4*	R5*	R6*			
	35								

^{*} in (mm)

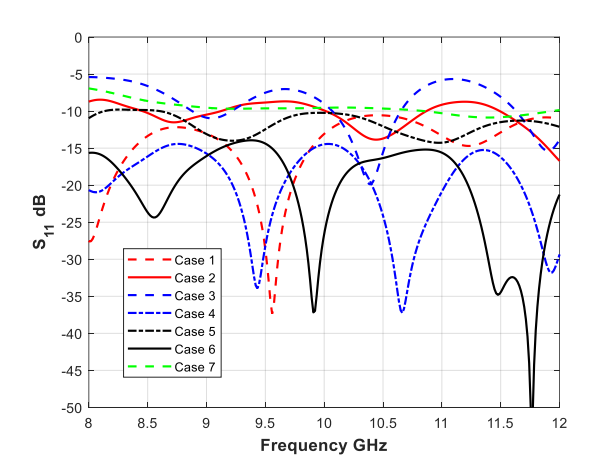
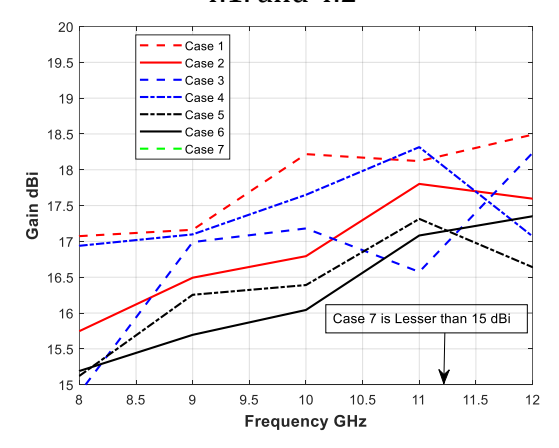


Figure 4.2 Simulated S_{11} Variations with frequency for the cases defined in table 4.1. and 4.2



 $\begin{tabular}{ll} \textbf{Figure 4.3} Simulated Gain variations with frequency for the Cases defined in table \\ 4.1 and 4.2 \end{tabular}$

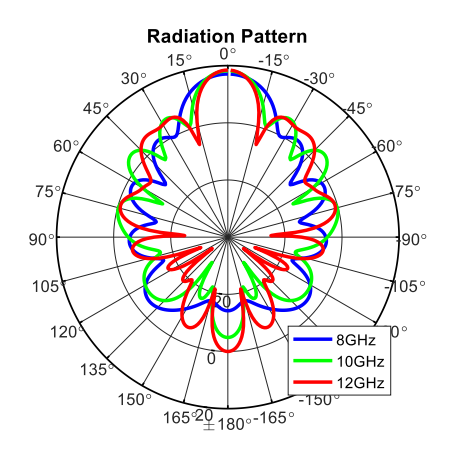
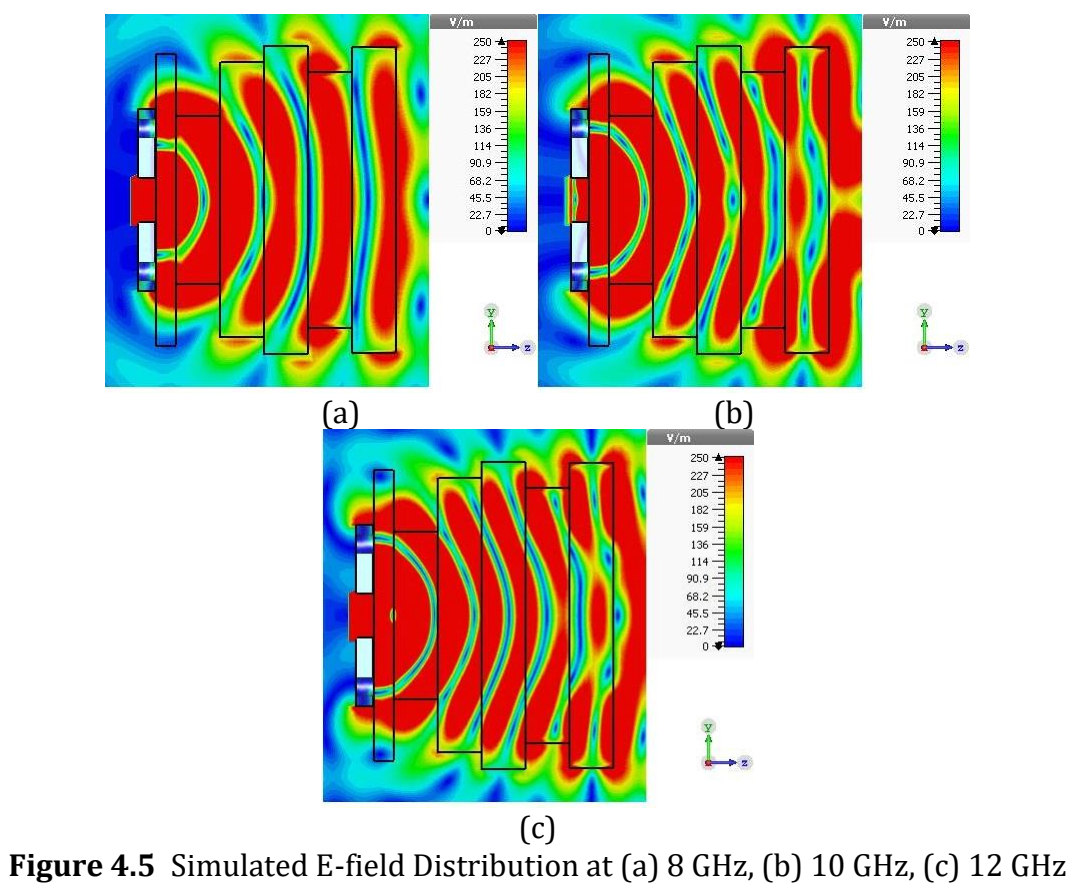


Figure 4.4 Simulated Radiation Patterns of Case 1



4.1.2 3D Printing Fabrication and Experimental Results of MLCDLA



Figure 4.6 Fabricated MLCDLA Model

In this section, a prototype of the proposed MLCDLA using 3D printing technology is presented. In Fig. 6, the 3D printed MLCDLA and measurement setup are shown. For the RF performance measurement of the proposed 3D printed MLCDLA, a Vector Network Analyzer with the measurement frequency range between 9 KHz and 13.5GHz Rohde - Schwarz RS Zvl13 , and "LB8180, 0.8-18 GHz broadband horn antenna" [124] are used.

Table 4.3 Simulated and Measured Radiation Characteristics of the Proposed MLCDLA

f (GHz)	S ₁₁ (dB)		Realized	Gain (dBi)	Side lobe level (dB)		
	Sim. Meas.		Sim.	Sim. Meas.		Meas.	
8	<-25	-20.2	17.1	16.3	-15.3	-12.8	
9	<-10	-9.8	17.2 16.6		-14.3	-14.8	
10	<-10	-17.4	18.2	17.5	-11.5	-11.4	
11	<-10	-12.3	18.1	17.6	-11.5	-11.2	
12	<-10	-14.8	18.5	18.4	-12.3	-12.1	

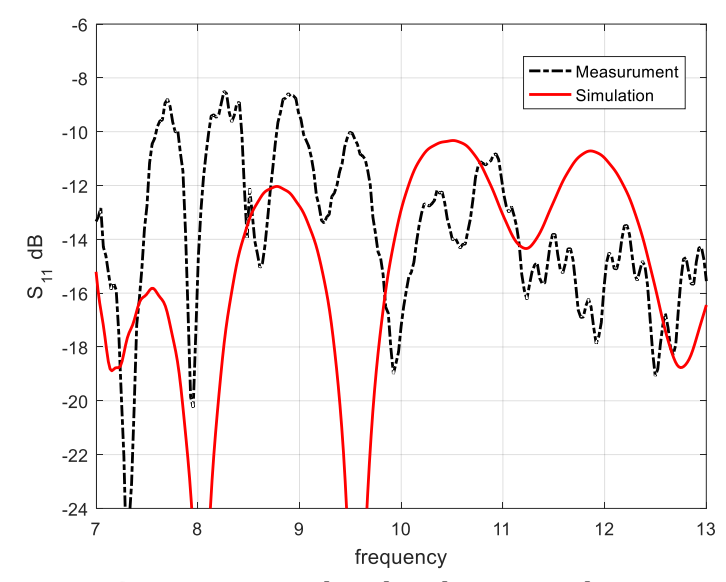


Figure 4.7 Simulated and Measured S₁₁

In Figs. 4.7-4.9 and Table 4.3, the measured and simulated results of return loss and radiation pattern of the proposed MLCDLA are given. The computed and measured S₁₁ of the MLCDLA are presented in Fig. 4.7. The fundamental reasons of the discrepancy between the simulation and measurement results can be the inherent material based fabrication tolerances, uncertainty in the dielectric constants of the incorporated cylindrical flat layers, calibration errors and RF cabling imposed multi resonance effects. The measured maximum gain and radiation pattern over the operation frequency band are denoted in Figs. 4.8-4.9. As it can be deduced from the figures, the measured and simulated results are in quite good agreement with the designed results of the proposed multilayer dielectric lens structure achieving minimum level of the measured gain as 16.3 dBi over the whole operation band. Thus, the proposed method using 3D printing technology for the design and fabrication of MLCDLA is an efficient solution for the realization of dielectric loaded antennas.

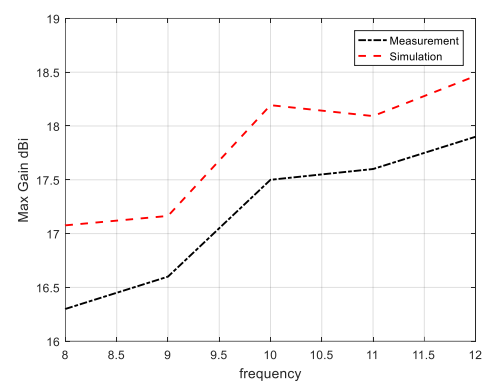


Figure 4.8 Maximum Gain Over the Operation Band

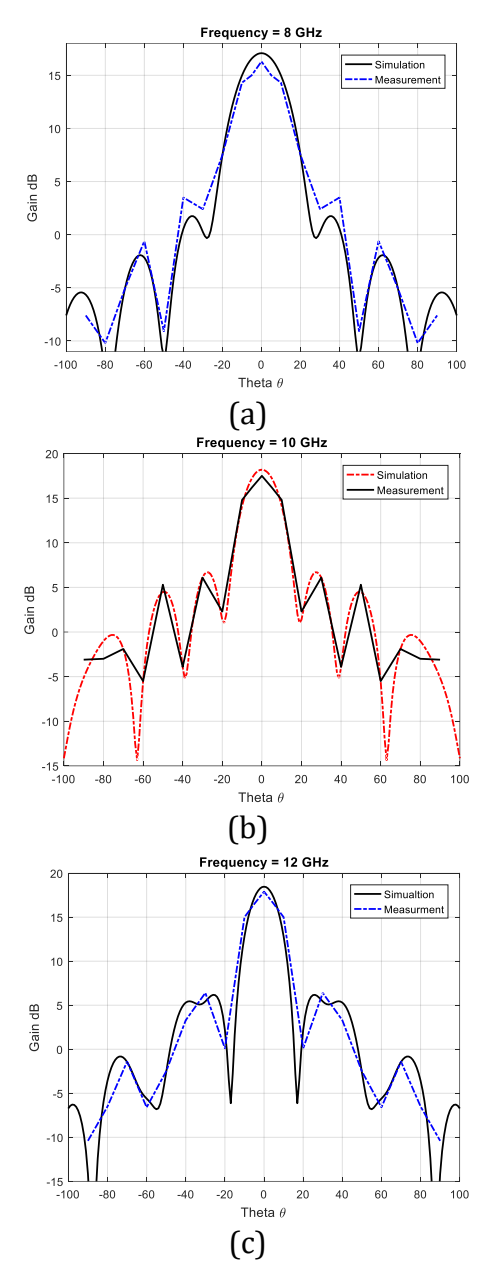


Figure 4.9 Measured Radiation Patterns of MLCDLA for ϕ =90° at (a) 8 GHz, (b) 10 GHz, (c) 12 GHz

Table 4.4 Comparison of Gain (dBi) Enhancements of the Typical Horn Modules in the Similar Bandwidth

		Gain(dBi) over operation band (GHz)						
	Dielectric size (mm)	8	9	10	11	12		
Here	35x35x62.6	16.3	16.6	17.5	17.6	18.4		
[120]	30×30×52.5	11.2	11.3	14	13.8	12.6		
[137]	279x244x159	16	18	14.8	17	15		
[138]	85.1x30.8x15.9	8.5	9	9	9	10		
[139]	90.7x210x210			17				
[140]	87.4x59.3x80	14	15.5	16.5	15	17		
[141]	74x81.5x60	10.7	11.3	8.2	10.2	9.8		

Furthermore, in Table 4.4, an RF performance comparison of the proposed MLCDLA antenna with the counterpart antennas in the literature operating within the similar operation band is shown. As concluded from the table, the proposed design is significantly better in comparison to the counterpart alternative designs in terms of both size and radiation characteristics

4.1.3 Discussion on Performance of Proposed MLCDLA

In study case, a high performance multi-layered cylindrical dielectric lens antenna is designed with the utilization of 3-D printing technology for fast, accurate and low cost complex prototyping. The experimental results point out 3-D printed antenna to have good reflection parameter characteristics of almost less than -10 dB within the operation frequency range of 8-12GHz with a good gain of 16-18 dBi. The measured and simulated results are in good agreement, which suggests the prototyped antenna to be suitable for X- band communication applications. Furthermore, an RF performance comparison of the proposed MLCDLA with the

counterpart designs operating in similar operation band is also made to prove the current design to be a better alternative to the fabricated designs in terms of both size and radiation characteristics. It can be concluded that the proposed 3-D printing method is not only a good fabrication solution to achieve the targeted performance characteristics but also a fast, low cost and effective method for prototyping the dielectric lens structures for the microwave applications.

5.1 3D Printed Wideband Flat Gain Multilayer Non-Uniform Reflectarray Antenna for X -Band Applications

Herein, design and realization of a wideband, flat gain Multi-layer Non-Uniform Reflect-Array (MNURA) using 3D printing technology is presented. Design optimization of the proposed MNURA has been achieved in the two stages: Firstly a 3D CST Microwave Studio based Multilayer Perceptron Neural Network (MLP NN) model establishes the reflection phase characteristic of the MNURA unit element as an accurate continuous function of the geometrical design parameters and dielectric constant. Then Differential Evolutionary Algorithm DEA is selected as a powerful optimization algorithm for determining the optimal geometrical design parameters and dielectric constant of MNURA over the X- band to have a large range, wideband and flat gain RA design. 3D printing technology has been used for prototyping of the proposed MNURA design. The prototyped antenna has a total size of 300x300 (mm), and its measured performance characteristics achieve a wideband flat gain of 23.2 dBi with a ripple level of almost 1.5dBi and return loss characteristic of less than -10 dB over the operation band of 8-12 GHz.

5.1.1 Design Process of Unit Cell Modelling

As it mentioned before, design of unit cell element is the first stage in the RA design process. As shown in Fig. 5.1, structure of the MNURA unit element consists of a dielectric layer (ε_r , h_1) an air gap (ε_r =1, h_2), and a copper layer as a covering layer and the MLP NN based Black –Box model of the unit element is given in Fig. 5.2 where reflection phase of the MNURA unit element is built up as a continuous function of the heights (h_1 , h_2), dielectric coefficient ε_r , and frequency f.

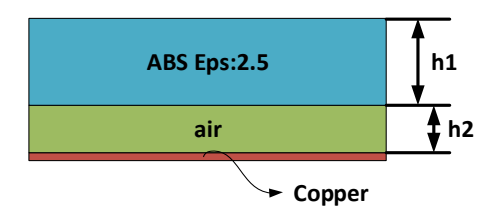


Figure 5.1 Unit Cell Structure of the MNURA h₁, h₂

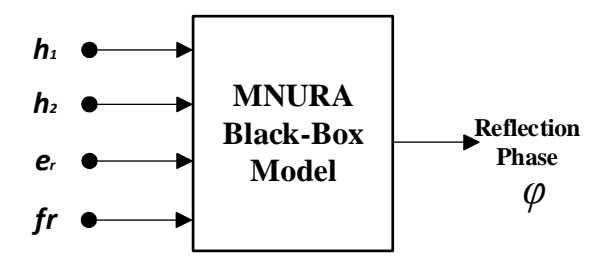


Figure 5.2 Black Box Model of the MNURA Unit Element

In in Table 5.1, lowest and uppermost limits of the design variables of the MNURA element are given. Thus, firstly, the training and test data set whose ranges are given in Table 5.1 will be obtained by 3D CST Microwave Studio using the H-wall simulator [68] for the MLP NN algorithm. In the second stage, the MLP NN algorithm parameters will be adjusted with respect to the accuracy criteria. Finally, the MLP NN model will be used with a powerful yet simple Differential Evolutionary Algorithm DEA [96-97] to determine the optimal MNURA unit element for a wide quasi-linear reflection response.

Table 5.1 Variables of the MNURA Unit Element

Parameter	Range	Step size	
h ₁ (mm)	0.5-15	0.5	
h ₂ (mm)	5-15	0.5	
ε _r	1.5-3	0.25	
Frequency (GHz)	8-12	0.5	
Total Sample	56700		

The data given in Table 5.1 are randomly being divided into two equally sized sets to be used as training and testing the MLP NN models having different number of hidden layer and neuron as given in Table 5.2 with the purpose of identifying the most optimum neural network in terms of efficiency and accuracy.

Table 5.2 User Defined Parameters of MLP NN Algorithms

MLP Model	User Defined Parameters
Case 1	1 hidden layer, with 5 neurons
Case 2	1 hidden layer, with 10 neurons
Case 3	1 hidden layer, with 15 neurons
Case 4	1 hidden layer, with 20 neurons
Case 5	2 hidden layer, with 5 and 10 neurons
Case 6	2 hidden layer, with 5 and 15 neurons,
Case 7	2 hidden layer, with 10 and 15 neurons
Case 8	2 hidden layer, with 15 and 20 neurons

^{*} Levenberg-Marquardt back-propagation are used for updating the weight and bias values of the models, all other parameters are taken as default.

Each of the MLP NN models given in Table 5.2 is optimized by the Levenberg – Marquardt back-propagation algorithm and tested for 10 runs that the resulted worst, best and mean performances given in Table 5.3.

Table 5.3 Performances of the MLP NN MODELS for 10 Runs Based on the Test Data Set

Case	Worst	Best	Mean
1	78.79	24.43	33.74
2	62.64	19.56	28.54
3	24.62	16.97	20.85
4	78.47	15.62	21.83
5	71.68	10.26	35.51
6	70.98	7.23	32.09
7	64.01	2.71	19.84
8	84.35	5.25	26.76

In Fig. 5.3, reflection phase variations of the Case 7 NN model are presented as compared with their CST simulations with respect to the heights (h_1 , h_2), dielectric coefficient ε_r , and frequency f.

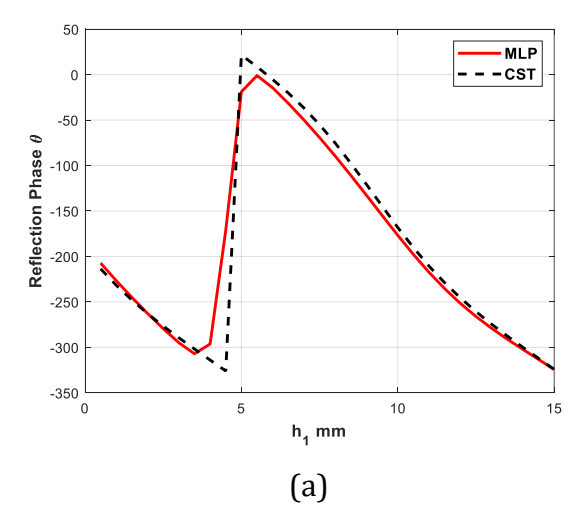


Figure 5.3 Reflection Phase Variations of MNURA Unit Element with (a) h_1 [h_2 =10mm, ϵ_r =2, f =10GHz], (b) h_2 [h_1 =10mm, ϵ_r =2, f =10GHz], (c) ϵ_r [h_1 =10mm, h_2 =10mm, f=10GHz], (d) f [h_1 =10mm, h_2 =10mm, ϵ_r =2]

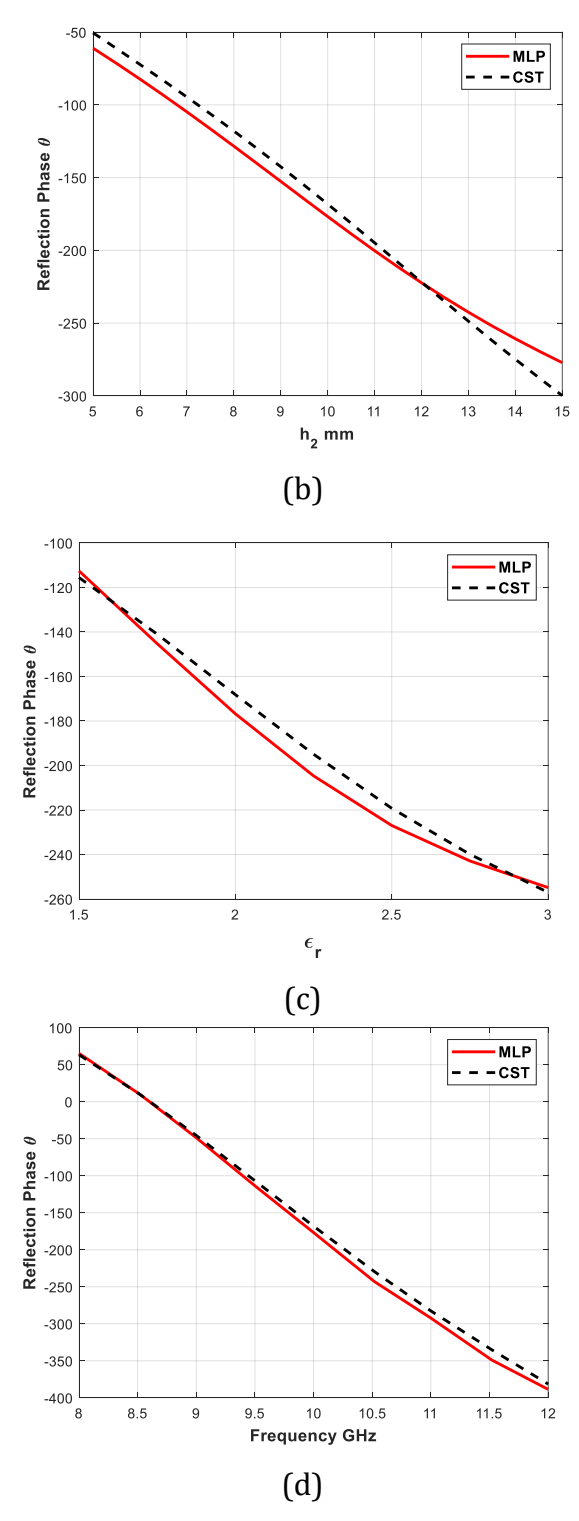


Figure 5.4 Reflection Phase Variations of MNURA Unit Element with (a) h_1 [h_2 =10mm, ϵ_r =2, f =10GHz], (b) h_2 [h_1 =10mm, ϵ_r =2, f =10GHz], (c) ϵ_r [h_1 =10mm, h_2 =10mm, f=10GHz], (d) f [h_1 =10mm, h_2 =10mm, ϵ_r =2] (continued)

As it can be seen from Table 5.3 and Fig. 5.3, Case 7 model of MNURA design has the best overall performance compared to the other MLP NN algorithms. Thus from hereon, all the optimization process in this work will use Case 7 model in Table 5.2.

5.1.2 Optimum MNURA Unit Cell

In this section, the optimum unit element is determined the geometry (h_1, h_2) in the substrate domain ϵr using Differential Evolutionary Algorithm so that a wide range, quasi-linear phasing characteristic can be obtained in a wide band within the X-band.

In the first stage, the optimal dielectric constant value ϵ_r and air gap height h_2 are determined using the following two steps: (I) The maximum reflection phase and dielectric height $(\phi_{max},j \; h_{1max},j)$ and the minimum reflection phase and dielectric height $(\phi_{minj}, \; h_{1minj})$ couples are obtained at each frequency within the $(\epsilon_{ri}, \; h_{2i})$ search domain by the equations given in Eqs. (5.1), (5.2). Then first condition for the optimal dielectric constant and air gap layer height $(\epsilon_r, \; h_2)$ couple can be obtained as having the wide phase difference as given in Eq. (5.3). Here, it should be noted that the variation range of the optimization variables $(\epsilon_{ri}, \; h_{2i})$ are defined with respect to Table 5.1.

$$f_{\max}(\epsilon_{ri}, h_{2i}, h_{1\max,j}, f_j) = \max_{\substack{0.5 \le h_1 \le 15 \\ \Delta h = 0.5}} \{ f(\epsilon_{ri}, h_{2i}, f_j, h_1) \}$$
 (5.1)

$$f_{\min}(\epsilon_{ri}, h_{2i}, h_{\min,j}f_{j}) = \min_{\substack{0.5 \in h_{1} \in 15\\ \Delta h = 0.5}} \{f(\epsilon_{ri}, h_{2i}, f_{j}, h_{1})\}$$
(5.2)

$$Cost_{1} = \frac{w_{1}}{\sum_{f_{i}=8}^{12} \left| f_{max}(\varepsilon_{ri}, h_{2i}, h_{1max,j}, f_{j}) - f_{min}(\varepsilon_{ri}, h_{2i}, h_{1min,j}, f_{j}) \right|}$$
(5.3)

(II) The second condition for the optimal (ϵ_r, h_2) couple is linearity of the reflection phase characteristic with respect to the dielectric height h_1 and frequency f for the flat gain over wideband. Similar to the previous step, for the defined range of the design variables, it is aimed to determining the optimal dielectric constant and air gap layer height (ϵ_r, h_2) couple within the (ϵ_{ri}, h_{2i}) search domain as follows:

$$Cost_{2} = w_{2} \left[\sum_{i=8}^{12} \frac{\Delta f(\varepsilon_{r_{i}}, h_{2_{i}}, f_{j}, h_{1})}{\Delta h_{1}} + \sum_{h_{1}=0.5}^{15} \frac{\Delta f(\varepsilon_{r_{i}}, h_{2_{i}}, f_{j}, h_{1})}{\Delta f_{i}} \right]$$
 (5.4)

where w_k (k=1, 2) are weighting coefficient of the cost functions.

Here an efficient optimization tool, Differential Evolutionary Algorithm (DEA) [96-97] is used for determining the optimal values of h₂ and dielectric constant εr based on Eqs.5.1-5.5. The user defined parameters of DEA are taken as: Maximum iteration=30, Population=50, Scale Factor=0.25, Cross-over=0.5. The optimal values of dielectric constant h₂ and height of the air layer h₂ with respect to the Cost functions in Eqs. 5.1-5.4, found as 2.2 and 13 mm.

In the second stage of design optimization, the required reflection phase for each unit element in MNURA model with 20x20 elements will be calculated based on the phase compensation proportional to the distance from the phase center of the feed-horn as well-known from the classical array theory [142]. In Table 5.4, the h_1 values of MNURA design for a feeding antenna with F/D ratio of (0.74) obtained from DEA with same user defined parameters in previous optimization process are presented. In the next section, the 3D EM simulation and experimental results of the 3D printed antenna will be studied.

Table 5.4 h₁ Values of Quadratic MNURA in (mm)

ID	1	2	3	4	5	6	7	8	9	10
1	13.6	10	11	10	2	1.4	7.2	20	1.2	4
2	10	4	8.6	3.2	2.8	1.2	1.6	1.5	1.5	4.2
3	11	8.6	6.4	6	1	1.2	1.2	20	1	10
4	10	3.2	6	1.2	1	1	2.8	1.7	8.4	1.2
5	2	2.8	1	1	2	15	20	17	3.2	10
6	1.4	1.2	1.2	1	15	20	8.4	1	1.8	1
7	7.2	1.6	1.2	2.8	20	8.4	11.5	3.2	2.6	1

Table 5.4 h₁ Values of Quadratic MNURA in (mm) (continued)

8	20	1.5	20	1.7	17	1	3.2	1	2	1
9	1.2	1.5	1	8.4	3.2	1.8	2.6	2	18	6.8
10	4	4.2	10	1.2	10	1	1	1	6.8	1

5.1.3 Simulated and Measured Results

In this section firstly the optimally selected design parameters in section II are used in order to form a large scale 20x20 MNURA antenna design in CST environment. In Fig. 5.4, 3D view of the full scale MNURA design alongside of its 3D radiation pattern at 10 GHz are presented. Also, in Fig. 5.5 and Table 5.5, the simulated return loss, polar radiation pattern, and side lobe level of MNURA design are given. As it can be seen from the Fig. 5.5 and Table 5.5, the simulated results suggested that the proposed MNURA design has high gain and low return loss characteristics over the operation band. In the next subsection, the 3D model full scale MNURA design will be prototyped by using 3D printing technology for measurements.

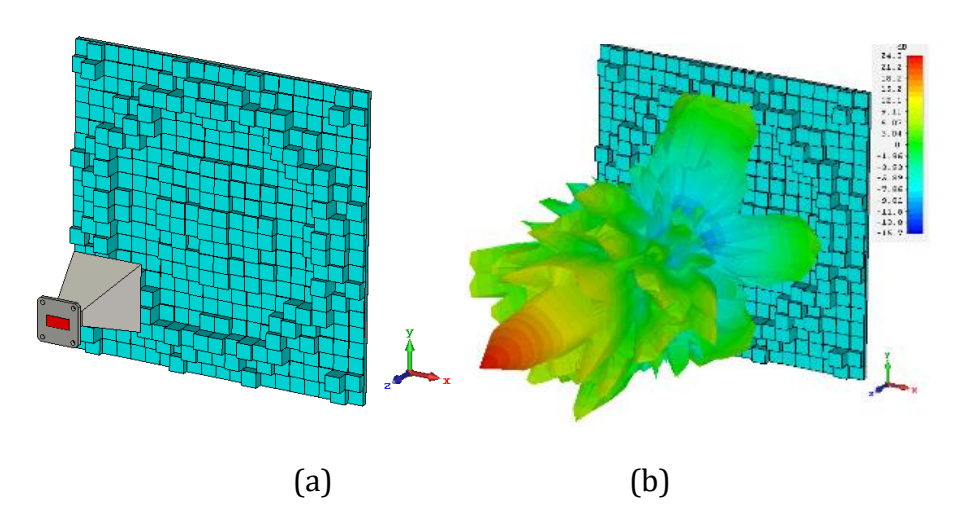


Figure 5.4 (a) 3D View, (b) Radiation Pattern @ 10 GHz of the 20x20 MNURA Antenna

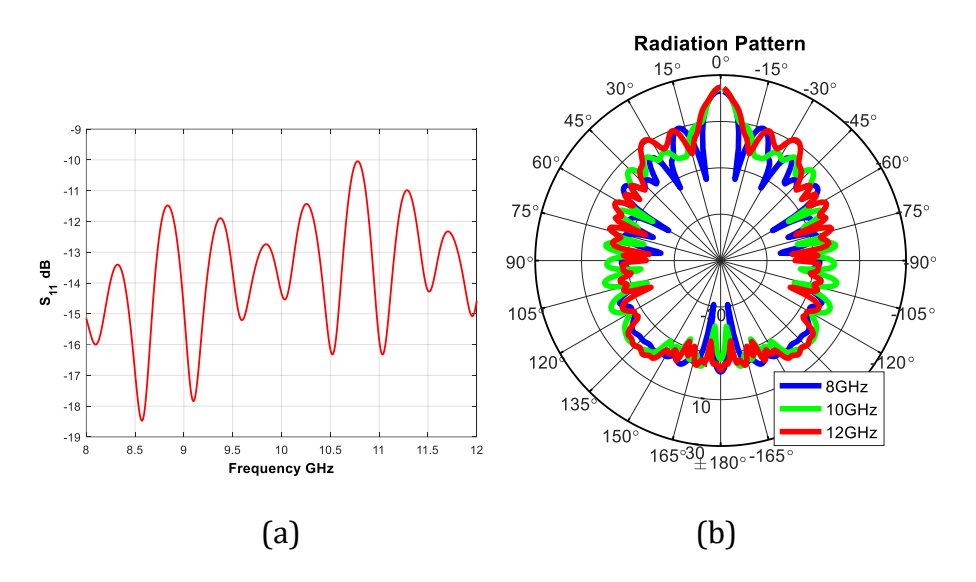


Figure 5.5 Simulated (a) Return Loss (b) Radiation Patterns

Table 5.5 Simulation Results of MNURA Antenna Design

f(GHz)	S ₁₁ (dB)	Realized Gain (dBi)	3dB (angle)	Side lobe level (dB)	
8	-15	23.2	7.70	-10.4	
9	-14.8	24.2	7.30	-12.9	
10	-14.1	24.3	6.20	-14.5	
11	-15.3	25.4	5.80	-16	
12	-14.6	24.9	5.30	-11.7	

As it mentioned before, fast and accurate prototyping process of microwave stages is at most importance for experimental based study cases. In this sub-section, 3D printing technology has been used for prototyping of the proposed MNURA antenna design. In order to prototype a design with a 3D printing process, stereolithography (STL) file format is needed. Here the stereolithography file of the proposed MNURA design has been taken from the CST microwave suite and given to CEL Robox® Micro [127]. "Polar White" PLA is taken as the dielectric substrate material of MNURA design with a dielectric constant of 2.2.

One of the advantages of 3D printers is their ability to adjust the infill rate of printed material within the structure that is mainly being used for creating design with lower weight values. However as it is studied in [122],[136], it is possible to adjust the dielectric properties of the 3D printed structure by increase or decreasing the infill rate of design as it is given in table 5.1. By using the Eq. (5.5) [122], the infill rate of the MNURA unit element is chosen as %56 which would provide a dielectric constant value of 2.2. In Figs. 5.6, the 3D printed MNURA design with its measurement setup has been presented.

$$\varepsilon_{\rm r} = -1.3 \times 10^{-6} \,{\rm x}^3 + 0.0374 \,{\rm x} + \frac{6.42}{\rm x} + 0.217$$
 (5.5)

where, i indicates the infill rate in %.

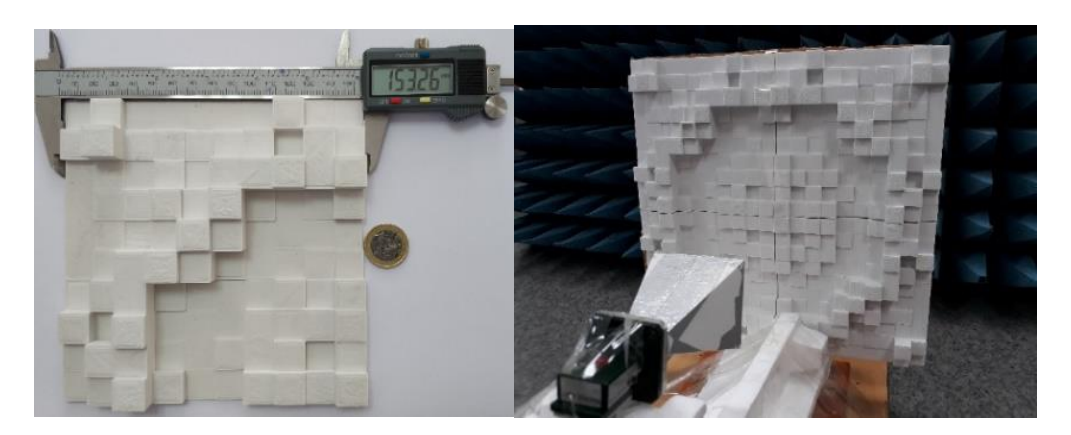


Figure 5.6 Prototyped 3D Printed NURA

In Figs 5.7-5.8, the measurement results of the prototyped MNURA design are presented. As it can be observed from the measurement results, both simulated and measured performance characteristics of the MNURA design are hand to hand, where the return loss (Fig. 5.8) has a measured characteristic of less than -10 dB over the operation band, and the gain (Fig. 5.9) has a flat characteristics of 23 dBi at 10 GHz with a ripple level of almost 1.5 over the operation band of 8-12 GHz. Furthermore, a comparison of the proposed MNURA design with the counterpart RA antenna design in the literature has been presented in Table 5.6. As it can be seen not only the proposed MNURA has a wide operation band but also it preserve its gain with a flat gain characteristics.

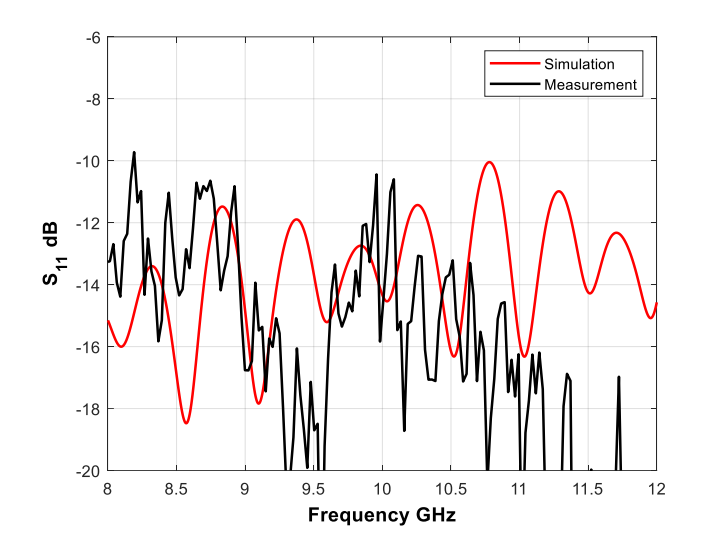


Figure 5.7 Measured NURA S₁₁ Characteristic

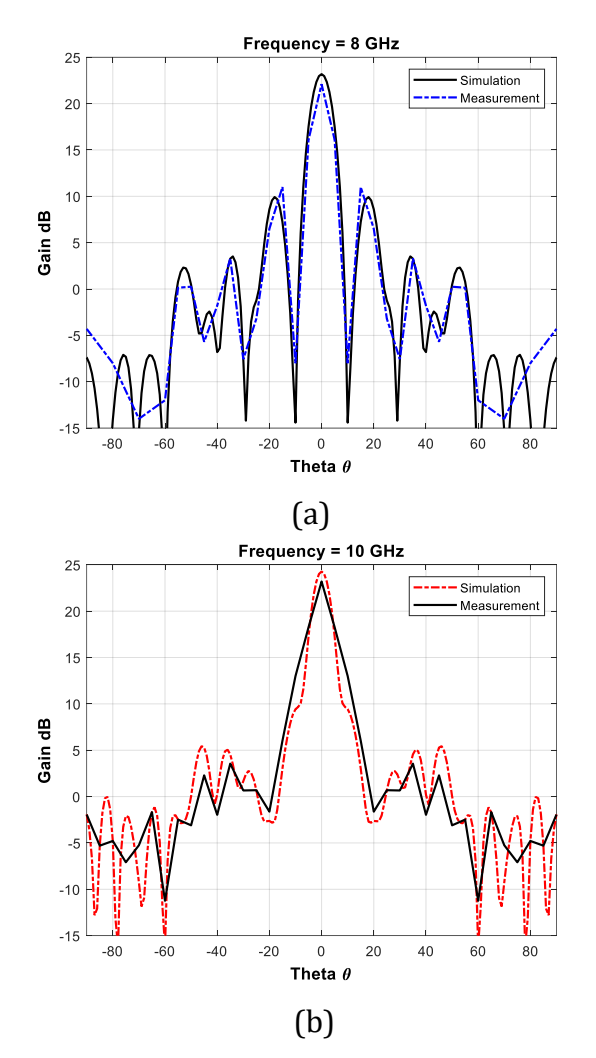


Figure 5.8 Measured Radiation Pattern of 3D Printed MNURA at (a) 8 GHz, (b) 10 GHz, (c) 12 GHz

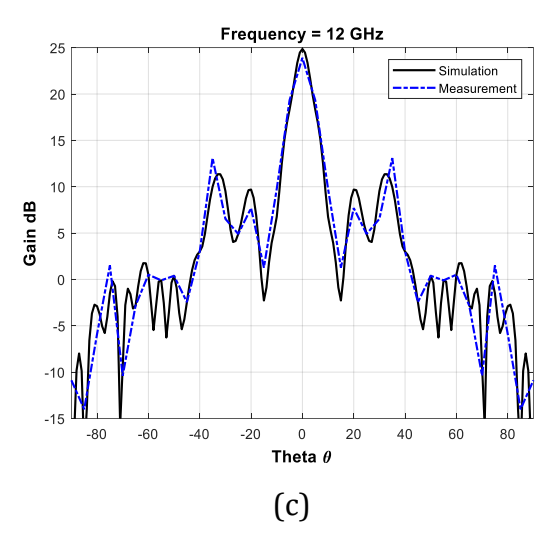


Figure 5.8 Measured Radiation Pattern of 3D Printed MNURA at (a) 8 GHz, (b) 10 GHz, (c) 12 GHz (continued)

Table 5.6 Performance Comparison of the Proposed MNURA with Counterpart

Designs in Literature

Model	Gain (dBi) over frequency (GHz)				псу	. Material	Die size	Dielectric
	8	9	10	11	12		(mm)	constant
MNURA	22.1	22.9	23.2	24.4	23.9	PLA	300x300	2.2
[143]	14.8	23	25.2	21	22.7	ERTALON	300x300	3
[144]		25	26.2	24.8		RO4003	300x300	4.13
[145]		22	25.2	23		Metal	420x420	
[146]			19	24	24	RT5880	200x200	2.2
[147]			30	31.4	31.2		400x400	2.17
[116]	19	20.8	22	19	16.4	ABS	300x300	2.5

5.1.4 Discussion on Performance of Proposed MNURA Design

In this study case, design and realization of a wide band, flat gain Multi-layer Non-Uniform Reflectarray antenna (MNURA) has been presented. Firstly, in order to obtain a linear reflection phase characteristic with respect to the geometrical design parameters, an AI based numerical model of the MNURA design has been created. After that, an optimization process driven by the obtained AI based model taken into consideration for determining the optimally selected geometrical design parameters. As a result, a large scale (20x20) MNURA design with simulated characteristics of flat gain of 24 dBi with 1.5 dBi ripple level, and a return loss characteristic of less than -10 dB over the operation band of 8-12 GHz had been obtained. Then for justification of simulated results, a 3D printer with fused deposition modelling (FDM) has been used for rapid prototyping of the proposed MNURA antenna design. The prototyped antenna design has a total size of 300x300 (mm), and its measured performance characteristics achieves a wideband flat gain of 23.2 dBi with a ripple level of almost 1.5dBi and return loss characteristic of less than -10 dB over the operation band of 8-12 GHz.

RESULTS AND DISCUSSION

As it mentioned before, developments in field of ITS, their applications are also expanded in many different applications such as Global Position System (GPS), Wireless network communication or mobile networks, RF or IR waves, data collection and transfers, long range communication systems for vehicles, automotive radar applications etc. with the ever increasing need of technology and complexity of systems and their environment, need of high performance microwave antenna designs are also increased. In this thesis, it was aimed to propose different antenna designs and novel design methodologies for answering the high performance antenna design demands for Intelligence Transportation Systems.

In this thesis, four different antenna designs had been studied, (I) Patch Loaded Traveling Wave Antenna (PLTWA), (II) SIW Microstrip patch antenna, (III) Multilayer dielectric loaded lens antenna, (IV) and a large scale Reflectarray antenna with flat gain characteristics.

I. The proposed PLTWA has a frequency dependent beam scanning within the operation band of 8 to 14 GHz with the dimensions of 30 × 130.0 mm that achieves a measured peak gain of 9.5 dBi and at 11 GHz with a main beam direction that is steerable with the range of (-65-15 degree). The comparison of the proposed PLTWA with counterpart works shows that the designs have a better performance. The proposed PLTWA is simple to design and fabricate and can be used in basic radar functions such as search, detection, tracking, guidance, and electron beam control applications. Also, the proposed PLTWA design can be easily adapted and realize in the higher mm-wave frequency band with the adequate performance.

- II. In third chapter of the thesis, design optimization and fabrication of a high performance SIW microstrip dual-band antenna had been presented. The SIW antenna design had been considered as a multi-objective multi-dimensional optimization problem to be solved using Differential Evolutionary Algorithm (DEA). The proposed dual band antenna had achieved a measured gain characteristic of 6.7 and 7 dB at 12 and 24 GHz respectively. Furthermore, for extending the performance enhancement of SIW structure a comparison analysis with recently published works with SIW designs in literature had been presented and as result, the proposed design optimization process has achieved an antenna model that not only have better or similar performance results (Gain and S₁₁), but also have realized this performance measure with smaller size compared to counterpart designs.
- III. In Chapter four, design and realization of high performance, low-cost, multilayered cylindrical dielectric lens antenna (MLCDLA) for X band applications had been studied. The proposed MLCDLA is designed was consisting of six layers and being fed through a conventional rectangular waveguide (WR90). These layers are in the form of cylindrical discs having different radii, thicknesses and made of a cheap polylactic acid material. These layers have also varying dielectric constant from 1.2 to 2.7 that are compatible for fused deposition modeling (FDM) based 3D-printing process. A prototype of MLCDLA is produced by using a FDM based 3D-printer. The antenna had achieved a measured gain of 16-18 dBi at X band with a good return loss of almost more than 10 dB. An RF performance comparison of the proposed MLCDLA antenna with the counterpart antennas in the literature operating within the similar operation band had been made and it is concluded that the proposed design is significantly better in comparison to the counterpart alternative designs in terms of both size and radiation characteristics. Thus, it can be concluded that the proposed novel design and prototyping method not only achieves the high radiation performance characteristics along X-band but also is a fast, low-cost, and effective method for prototyping dielectric lens structures for the microwave applications.

IV. In Chapter 5 of the thesis, design and realization of a 3D Printed Wideband Flat Gain Multilayer Non-Uniform Reflectarray Antenna using ANN and Metaheuristic optimization algorithm had been studied. The prototyped antenna has a total size of 300 × 300 (mm), and its measured performance characteristics achieve a wideband flat gain of 23.2 dBi with a ripple level of almost 1.5 dBi and return loss characteristic of less than −10 dB over the operation band of 8 to 12 GHz. Furthermore, a comparison of the proposed MNURA design with the counterpart RA antenna design in the literature has been done and as a result, the proposed MNURA not only has a wide operation band but also it preserves its gain with a flat gain characteristics.

Thus, in this thesis by using powerful 3D EM simulation tools, Artificial Intelligence based algorithms such as Artificial Neural networks and meta-heuristic optimizers, and 3D printing technology design of high performance and low cost antenna stages for applications of Intelligence Transportation Systems had been achieved.

- [1] H. Tüydeş Yaman, "Akıllı Ulaşım Sistemleri tanımı ve kapsamı", Akıllı Ulaşım ve Güvenlik Sistemleri dergisi, s.54, 2014.
- [2] HGM, 2018, Akıllı Ulaşım Sistemleri (AUS), Haberleşme Genel Müdürlüğü, http://hgm.ubak.gov.tr/tr/sayfa/49, erişim tarihi: 10.09.2018.
- [3] S. An, B. Lee and D. Shin, "A Survey of Intelligent Transportation Systems," *2011* Third International Conference on Computational Intelligence, Communication Systems and Networks, Bali, 2011, pp. 332-337, doi: 10.1109/CICSyN.2011.76.
- [4] M. Maekawa, "ITS (Intelligent Transportation Systems) Solutions", NEC J. of Adv. Tech., pp. 194–199, 2004.
- [5] M. Mehta, M. Guinan, "The Utilisation of Multi-Antenna Enhanced Mobile Broadband Communications in Intelligent Transportation Systems," *2007 7th International Conference on ITS Telecommunications*, Sophia Antipolis, pp. 1-4, 2007, doi: 10.1109/ITST.2007.4295906.
- [6] J. Zhu, Y. Yang, S. Li, S. Liao and Q. Xue, "Dual-Band Dual Circularly Polarized Antenna Array Using FSS-Integrated Polarization Rotation AMC Ground for Vehicle Satellite Communications," in IEEE Transactions on Vehicular *Technology*, vol. 68, no. 11, pp. 10742-10751, Nov. 2019, doi: 10.1109/TVT.2019.2938266.
- [7] H. Bayer, A. Krauss, T. Zaiczek, R. Stephan, O. Enge-Rosenblatt and M. A. Hein, "Ka-Band User Terminal Antennas for Satellite Communications [Antenna Applications Corner]," in *IEEE Antennas and Propagation Magazine*, vol. 58, no. 1, pp. 76-88, Feb. 2016, doi: 10.1109/MAP.2015.2501244.
- [8] S. Lindenmeier, I. Goncharova, S. Hastürkoğlu and M. B. Diez, "Antennas for terrestrial communication in vehicles and their interaction with antennas for satellite services," 2017 IEEE-APS Topical Conference on Antennas and Propagation in Wireless Communications (APWC), Verona, 2017, pp. 334-337, doi: 10.1109/APWC.2017.8062319.
- [9] R. Bishop, "Application Areas",in Intelligent Vehicle Technology and Trends, Artech House ITS Library, pp. 25 37, 2005.
- [10] R. Lachner, "Development Status of Next Generation Automotive Radar in EU", ITS Forum, Tokyo, 2009.
- [11] G. L. Charvat, "Small and Short-Range Radar Systems", CRC Press, 2014.
- [12] A. Kajiwara, "UltraWideband Automotive Radar",in Advances in Vehicular Networking Technologies, pp. 103 122, 2011.
- [13] https://www.rfpage.com/applications-of-millimeter-waves-future, (2020, November 18).

- [14] Kishore, N., Upadhyay, G., Prakash, A., & Tripathi, V. S.. (2018). Millimeter Wave Antenna for Intelligent Transportation Systems Application. Journal of Microwaves, Optoelectronics and Electromagnetic Applications, 17(1), 171-178.
- [15] Meinel, H., (2014). "Evolving Automotive Radar from the very beginnings into the future", The 8th European Conference on Antennas and Propagation, 6-11 Nisan 2014, Stuttgart.
- [16] Gu C, Gao S, Sanz-Izquierdo B, et al. 3-d coverage beam-scanning antenna using feed array and active frequency-selective surface. IEEE Trans Antennas Propag. 2017;65(11):5862-5870.
- [17] Zhang S, Huff GH, Feng J, Bernhard JT. A pattern reconfigurable microstrip parasitic array. IEEE Trans Antennas Propag. 2004;52(10):2773-2776.
- [18] Ding X, Wang B-Z. A novel wideband antenna with reconfigurable broadside and endfire patterns. IEEE Antennas Wireless Propag Lett. 2013;12: 995-998.
- [19] Zhu HL, Cheung SW, Yuk TI. Mechanically pattern reconfigurable antenna using metasurface. IET Microw Antennas Propag. 2015;9(12):1331-1336.
- [20] Ding C, Guo YJ, Qin PY, Bird TS, Yang Y. A defected microstrip structure (DMS)-based phase shifter and its application to beamforming antennas. IEEE Trans Antennas Propag. 2014;62(2):641-651.
- [21] Edalati A, Denidni TA. Frequency selective surfaces for beam-switching applications. IEEE Trans Antennas Propag. 2013;61(1):195-200.
- [22] Rodrigo D, Cetiner BA. Frequency, radiation pattern and polarization reconfigurable antenna using a parasitic pixel layer. IEEE Trans Antennas Propag. 2014;62(6):3422-3427.
- [23] Pringle LN, Harms PH, Blalock SP, et al. A reconfigurable aperture antenna based on switched links between electrically small metallic patches. IEEE Trans Antennas Propag. 2004;52(6):1434-1445.
- [24] Kovitz JM, Rajagopalan H, Rahmat-Samii Y. Design and implementation of broadband MEMS RHCP/LHCP reconfigurable arrays using rotated E-shaped patch elements. IEEE Trans Antennas Propag. 2015;63(6):2497-2507.
- [25] Gianvittorio JP, Rahmat-Samii Y. Reconfigurable patch antennas for steerable reflectarray applications. IEEE Trans Antennas Propag. 2006;54(5):1388-1392.
- [26] Petit L, Dussopt L, Laheurte JM. MEMS-switched parasitic-antenna array for radiation pattern diversity. IEEE Trans Antennas Propag. 2006;54(9): 2624-2631.
- [27] Qin PY, Guo YJ, Ding C. A beam switching quasi-Yagi dipole antenna. IEEE Trans Antennas Propag. 2013;61(10):4891-4899.
- [28] Zhang X, Tian M, Zhan A, Liu Z, Liu H. A frequency reconfigurable antenna for multiband mobile handset applications. Int J RF Microw Comput Aided Eng. 2017;27:e21143. https://doi.org/10.1002/mmce.21143

- [29] Saraswat K, Harish AR. A polarization reconfigurable CPW fed monopole antenna with L-shaped parasitic element. Int J RF Microw Comput Aided Eng. 2018;28:e21285. https://doi.org/10.1002/mmce.21285
- [30] Li K, Cai Y-M, Yin Y, Hu W. A Wideband E-plane Pattern Reconfigurable Antenna with Enhanced Gain. Int J RF Microw Comput Aided Eng. 2018;e21530. https://doi.org/10.1002/mmce.21530
- [31] Bagheroghli H, Zaker R.Double triangular monopole-like antenna with reconfigurable single/dual-wideband circular polarization. IntJ RF Microw Comput Aided Eng. 2018;28:e21267.https://doi.org/10.1002/mmce.21267
- [32] M. A. Belen, "Traveling-wave microstrip array antenna using substrate integrated wavequide," 2018 22nd International Microwave and Radar Conference (MIKON), Poznan, 2018, pp. 37-40. doi: 10.23919/MIKON.2018.8405228
- [33] W. Menzel, "A new travelling-wave antenna in microstrip," AEU, vol. 33, no. 4, pp. 137–140, 1979.
- [34] G. V. Trentini, "Partially reflecting sheet arrays," IRE Trans. Antennas Propag., vol. AP-4, no. 4, pp. 666–671, Oct. 1956.
- [35] D. R. Jackson and A. A. Oliner, "A leaky-wave analysis of the high-gain printed antenna configuration," IEEE Trans. Antennas Propag., vol. 36, no. 7, pp. 905–910, Jul. 1988.
- [36] R.Gardelli, M. Albani, and F. Capolino, "Array thinning by using antennas in a Fabry-Perot cavity for gain enhancement," IEEE Trans. Antennas
- Propag., vol. 54, no. 7, pp. 1979–1990, Jul. 2006.
- [37] S. K. Podilchak, A. P. Freundorfer, Y. M. M. Antar, and S. F. Mahmoud, "Dielectric based leaky-wave antenna for high gain using a printed surfacewave source," Electron. Lett., vol. 46, no. 23, pp. 1537–1539, Nov. 2010.
- [38] F. Scattone, M. Ettorre, F. Fuchs, R. Sauleau, and N. J. G. Fonseca, "Synthesis procedure for thinned leaky-wave-based phased arrays with reduced number of elements," IEEE Trans. Antennas Propag., vol. 64, no. 2, pp. 582–590, Feb. 2015.
- [39] R. Sauleau, P. Coquet, D. Thouroude, J.-P. Daniel, and T. Matsui, "Radiation characteristics and performance of millimeter-wave horn-fed Gaussian beam antennas," IEEE Trans. Antennas Propag., vol. 51, no. 3, pp. 378–387, Mar. 2003.
- [40] A. Neto, M. Ettorre, G. Gerini, and P. De Maagt, "Leaky-wave enhanced feeds for multi-beam reflectors to be used for telecom satellite based links," IEEE Trans. Antennas Propag., vol. 60, no. 1, pp. 110–120, Jan. 2012.
- [41] F. Scattone, M. Ettorre, R. Sauleau, N. T. Nguyen, and N. J. G. Fonseca, "Optimization procedure for planar leaky-wave antennas with flat-topped radiation patterns," IEEE Trans. Antennas Propag., vol. 63, no. 12, pp. 5854–5859, Dec. 2015.

- [42] F. Scattone, "Phased array antenna with significant reduction of active controls," Ph.D. dissertation, Dept. Antennes Dispositifs Hyperfr'equences, Universit'e de Rennes 1, Rennes, France, 2015.
- [43] J. L. Gomez-Tornero, A. T. Martinez, D. C. Rebenaque, M. Gugliemi, and A. Alvarez-Melcon, "Design of tapered leaky-wave antennas in hybrid waveguide-planar technology for millimeter waveband applications," IEEE Trans. Antennas Propag., vol. 53, no. 8, pp. 2563–2577, Aug. 2005.
- [44] C. A. Balanis, Modern Antenna Handbook. New York, NY, USA: Wiley, 2008.
- [45] Belen, M, MAHOUTI, P, (2018). X Band Radar Sistemleri için Mikroşerit Yürüyen Dalga Anten Tasarımı. Iğdır Üniversitesi Fen Bilimleri Enstitüsü Dergisi, 8 (4), 87-96. DOI: 10.21597/jist.415458
- [46] Lee D, Lim S. Leaky-wave antenna design using quarter-mode substrate-integrated waveguide. Microw Opt Technol Lett. 2015; 57(5):1234–1236.
- [47] Lyu Y-L, Liu X-X, Wang P-Y, et al. Leaky-wave antennas based on noncutoff substrate integrated waveguide supporting beam scanning from backward to forward. IEEE Trans Antennas Propagat. 2016;64(6):2155–2164.
- [48] Prasad CS, Biswas A, Akhtar, MJ. Leaky wave antenna for wide range of beam scanning through broadside in dielectric image line environment. Microw Opt Technol Lett. 2018; 60:1707–1713.
- [49] M. Bozzi, L. Perregrini, K. Wu, P. Arcioni, "Current and Future Research Trends in Substrate Integrated Waveguide Technology", Radioengineering, 18(2), 2009.
- [50]W. Jiang, K. Huang, C. Liu, "Ka-Band Dual-Frequency Single-Slot Antenna Based on Substrate Integrated Waveguide", IEEE Antennas and Wireless Propagation Letters, 17(2), 221-224, 2017.
- [51]T. Cheng, W. Jiang, S. Gong, Y. Yu, "Broadband SIW cavity-backed modified dumbbell-shaped slot antenna", IEEE Antennas and Wireless Propagation Letters, 18(5), 936-940, 2019.
- [52]M. A. Belen, P. Mahouti, A. Çalışkan, A. Belen, "Modeling and Realization of Cavity-Backed Dual-Band SIW Antenna" Applied Computational Electromagnetics Society Journal, Vol. 32, No. 11, 974-978, 2017.
- [53]A. Belen, F. Güneş, "Design and Realization of Dual Band microstrip SIW antenna", Sigma Journal of Engineering and Natural Sciences, Vol.37(4), pp.1083-1092, 2019
- [54] M.A. Belen, F. Güneş, A. Çalışkan, P. Mahouti, S. Demirel, A. Yıldırım, "Microstrip SIW Patch Antenna Design for X Band Application", MIKON 21st International Conference on Microwaves, Radar and Wireless Communications, Krakow POLAND, 2016.
- [55] J. Lacik, "Circularly polarized SIW square ring-slot antenna for X-band applications", Microw. Opt. Technol. Lett., 54: 2590–2594, 2012
- [56] S. Moitra, P.S. Bhowmik, "Effect of Various Slot Parameters in Single Layer Substrate Integrated Waveguide (SIW) Slot Array Antenna for Ku-Band

- Applications", Applied Computational Electromagnetics Society Journal, 30(8), 2015.
- [57]N. Tiwari, T.R Rao, "Antipodal Linear Tapered Slot Antenna with Dielectric Loading Using Substrate Integrated Waveguide Technology for 60 GHz Communications" Applied Computational Electromagnetics Society Journal, 32(4), 2017.
- [58]E. Baghernia, M.H. Neshati, "Development of a Broadband Substrate Integrated Waveguide Cavity Backed Slot Antenna Using Perturbation Technique" Applied Computational Electromagnetics Society Journal, 29(11), 2014.
- [59] Schoenlinne B. R, Wu X., Ebling J.P., Eleftheriades G.V., and Rebeiz G.M., "Widescan spherical-lens antennas for automotive radars," IEEE Trans Microwave Theory Tech 50 (2002), 2166–2175.
- [60] Fuchs B., Lafond O., Rondineau S., Himdi M., and Coq L. Le, "Off-axis performances of half Maxwell fish-eye lens antennas at 77GHz," IEEE Trans Antennas Propag 55 (2007), 479–482.
- [61] Costa J.R., Fernandes C.A., Godi G., Sauleau R., Coq L. Le, and Legay H., "Compact Ka-band lens antennas for LEO satellites," IEEE Trans Antennas Propag 56 (2008), 1251–1258.
- [62] C.A. Fernandes, Shaped dielectric lenses for wireless millimeter-wavecommunications, IEEE Antennas Propag Mag 41 (1999), 141–150.
- [63] J. R. Risser, Microwave Antenna Theory and Design. New York, NY, USA: McGraw-Hill, 1949.
- [64] B. Chantraine-Bares, R. Sauleau, L. L. Coq, and K. Mahdjoubi, "A new accurate design method for millimeter-wave homogeneous dielectric substrate lens antennas of arbitrary shape," IEEE Trans. Antennas Propag., vol. 53, no. 3, pp. 1069–1082, Mar. 2005.
- [65] Kock W. E., "Metallic delay lens," Bell System Tech. J., vol. 27, pp. 58–82, Jan. 1948.
- [66] Kock W. E., "Metal lens antennas," Proc. IRC, vol. 34, no. 11, pp. 826–836, Nov. 1946.
- [67] Berry, D. G., Malech, R. G., Kennedy, W. A., 1963. The Reflectarray Antenna. IEEE Trans. Antennas Propag., vol. 11, no. 6, pp. 645–651.
- [68] Phelan, H. R., 1977. Spiral phase Reflectarray for Multitarget Radar. Microw. J., vol. 20, pp. 67–73.
- [69] Huang, J., Encinar, J. A., 2007. Reflectarray Antennas. IEEE Press.
- [70] Munson, R. E., Haddad, H., 1987. Microstrip Reflectarray for Satellite Communication and RCS Enhancement and Reduction. U.S. Pat. 4684952, Washington, D.C.
- [71] Huang, J., 1991. Microstrip Reflectarray. IEEE AP S/URSI Symp. London, Canada, pp. 612–615.

- [72] Pozar, D. M., Metzler, M., 1993. A. Analysis of a Reflectarray Antenna Using Microstrip Patches of variable Size. Electron. Lett., vol. 29, no. 8, pp. 657–658.
- [73] Kelkar, A., 1995. FLAPS: Conformal Phased Reflecting Surfaces. Proc. IEEE Natl. Radar Conf., Los Angeles, Calif., pp. 58 62.
- [74] Guo, Y. J., Barton, S. K., 1995. Phase Correcting Zonal Reflector Incorporating Rings. IEEE Trans. Antennas Propag., vol. 43, no. 4, pp. 350–355.
- [75] Huang, J., Pogorzelski, R. J., 1998. A Ka Band Microstrip Reflectarray with Elements having variable Rotation Angles. IEEE Trans. Antennas Propag., vol. 46, no. 5, pp. 650–656.
- [76] D. Rodrigo, L. Jofre and J. Perruisseau-Carrier, "Unit Cell for Frequency-Tunable Beamscanning Reflectarrays," in IEEE Transactions on Antennas and Propagation, vol. 61, no. 12, pp. 5992-5999, Dec. 2013, doi: 10.1109/TAP.2013.2281375.
- [77] Güneş, F., Nesil, S., Demirel, S., 2013. Design and Analysis of Minkowski Reflectarray Antenna Using 3-D CST Microwave Studio-Based Neural Network Model with Particle Swarm Optimization. International Journal of RF and Microwave Computer-Aided Engineering, vol.23, no.2, pp.272-284.
- [78] Güneş, F., Demirel, S., Nesil, S. 2014. A Novel Design Approach to X-Band Minkowski Reflectarray Antennas using the Full-Wave EM Simulation-based Complete Neural Model with a Hybrid GA-NM Algorithm. Radioengineering, vol. 23, No. 1.
- [79] Pozar, D. M., Targonski, S. D., Pokuls, R., 1999. A Shaped-Beam Microstrip Patch Reflectarray. IEEE Trans. Antennas Propag., vol. 47, no. 7, pp. 1167–1173.
- [80] Encinar, J. A., Zornoza, J. A., 2004. Three-Layer Printed Reflectarrays for Contour Beam Space Applications. IEEE Trans. Antennas Propag., vol. 52, pp. 1138–1148.
- [81] Pozar, D. M., 2003. Bandwidth of Reflectarrays. Electron. Lett., vol. 39, no. 21, pp. 1490 1491.
- [82] Encinar, J. A., Zornoza, J. A., 2003. Broadband Design of Three-Layer Printed Reflectarrays. IEEE Trans. Antennas Propag., vol. 51, pp. 1662–1664.
- [83] Encinar, J. A., 2001. Design of Two-Layer Printed Reflectarray Using Patches of Variable Size," IEEE Trans. Antennas Propag., vol. 49, pp. 1403–1410..
- [84] Mahouti, P., 2020. Application of artificial intelligence algorithms on modeling of reflection phase characteristics of a nonuniform reflectarray element. International Journal of Numerical Modelling: Electronic Networks, Devices and Fields, 33(2), e2689.
- [85] M. Zhou, S. B. Sorensen, O. S. Kim, E. Jorgensen, P. Meincke and O. Breinbjerg, "Direct Optimization of Printed Reflectarrays for Contoured Beam Satellite Antenna Applications," in *IEEE Transactions on Antennas and Propagation*, vol. 61, no. 4, pp. 1995-2004, April 2013, doi: 10.1109/TAP.2012.2232037.
- [86] H. Chou and J. W. Liu, "Synthesis and Characteristic Evaluation of Convex Metallic Reflectarray Antennas to Radiate Relatively Orthogonal Multibeams,"

- in *IEEE Transactions on Antennas and Propagation*, vol. 66, no. 8, pp. 4008-4016, Aug. 2018, doi: 10.1109/TAP.2018.2841422.
- [87] Huang, J. 1990. Microstrip reflectarray antenna for the SCANSCAT radar application.
- [88] Pozar, D. M., Targonski S. D., 1997. Syrigos H. Design of millimeter wave microstrip reflectarrays. IEEE transactions on antennas and propagation 45(2): 287–296.
- [89] F. Glover, G.A. Kochenberger, "Handbook of metaheuristics" Springer, International Series in Operations Research & Management Science, 2003.
- [90] E. G. Talbi, "Metaheuristics: from design to implementation." Wiley, 2009.
- [91] F. Güneş, S. Demirel, P. Mahouti, "Design of A Front– End Amplifier For The Maximum Power Delivery And Required Noise By HBMO With Support Vector Microstrip Model". Radioengineering, 23, 2014.
- [92] F. Güneş, S. Demirel, P. Mahouti,, "A simple and efficient honey bee mating optimization approach to performance characterization of a microwave transistor for the maximum power delivery and required noise", Int. J. Numer. Model. 2015, doi: 10.1002/jnm.2041.
- [93] K. Güney, M. Onay, "Bees Algorithm for Design of Dual- Beam Linear Antenna Arrays with Digital Attenuators and Digital Phase Shifters". Int J RF and Microwave CAE, 18:337–347, 2008.
- [94] A. Galehdar, D.V. Thiel, A. Lewis, M. Randall, "Multi objective Optimization for Small Meander Wire Dipole Antennas in a Fixed Area Using Ant Colony System". Int J RF and Microwave CAE, 19, 592–597, 2009.
- [95] A. Yildirim, F. Güneş, M. A. Belen, "Differential Evolution Optimization Applied to the Performance Analysis of a Microwave Transistor "journal: sigma journal of engineering and natural sciences, 8(2), pp.135-144, 2017.
- [96] F. Güneş, M.A. Belen, P. Mahouti, "Competitive evolutionary algorithms for building performance database of a microwave transistor" Int J Circ Theor Appl. Vol.46, pp. 244–258, 2018.
- [97] K. Price, R. M. Storn, J. A. Lampinen, "Differential Evolution", Springer-Verlag Berlin Heidelberg, 2005.
- [98] Giannini, F., Leuzzi, G., Orengo, G., Albertini, M, 2002. Small-signal and large-signal modeling of active devices using CAD-optimized neural networks. Int J RF Microwave Computer-Aided Eng 12, 71–78.
- [99] Marinkovic, Z. D., Markovic, V. V., 2005. Temperature-dependent models of low-noise microwave transistors based on neural networks. Int J RF Microwave Computer-Aided Eng 15, 567–577.
- [100] Krishna, D., Narayana, J., Reddy, D. 2008. ANN Models for Microstrip Line Synthesis and Analysis. World Academy of Science, Engineering and Technology, International Science Index 22, International Journal of Electrical, Computer, Energetic, Electronic and Communication Engineering, 2(10), 2343 2347.

- [101] Güneş F., Nesil S., Demirel S., 2013. Design and Analysis of Minkowski Reflectarray Antenna Using 3-D CST Microwave Studio-Based Neural Network Model with Particle Swarm Optimization. Int J RF Microwave Computer-Aided Eng, vol.23, pp.272-284.
- [102] M. Zhou, S. B. Sørensen, O. S. Kim, E. Jørgensen, P. Meincke and O. Breinbjerg, "Direct Optimization of Printed Reflectarrays for Contoured Beam Satellite Antenna Applications," in *IEEE Transactions on Antennas and Propagation*, vol. 61, no. 4, pp. 1995-2004, April 2013, doi: 10.1109/TAP.2012.2232037.
- [103] Güneş F., Torpi H., and Gürgen F., 1998. A multidimensional signal-noise neural network model for microwave transistors", IEE Proc Circ Devices Syst. 145, 111–117.
- [104] Zhang, Q.J., Gupta, K.C., 2000. Neural Networks for RF and Microwave Design. Artech House, Boston.
- [105] Suntives, A., Hossain, M. S., Ma, J., Mittra, R. Veremey, V., 2001. Application of artificial neural network models to linear and nonlinear RF circuit modeling. Int J RF and Microwave Comp Aid Eng, 11: 231-247. doi:10.1002/mmce.1028.
- [106] Hammoodi, A.I., Milanova, M., Raad, H., 2018. Elliptical Printed Dipole Antenna Design using ANN Based on Levenberg–Marquardt Algorithm. Advances in Science, Technology and Engineering Systems Journal, vol. 3, no. 5, pp. 394-397.
- [107] Karaboga, D., Guney, K., Sağiroğlu, S., Erler, M., 1999. Neural computation of resonant frequency of electrically thin and thick rectangular microstrip antennas. IEE Proc Microwave Antennas Propag 146, 155–159.
- [108] Mishra, R.K., Patnaik, A., 1998. Neural network-based CAD model for the design of square patch antennas, IEEE Trans Antennas propag. 46, 1890–1891.
- [109] Rosenblatt, F., 1961. Principles of Neurodynamics: Perceptrons and the Theory of Brain Mechanisms. Spartan Books, Washington DC.
- [110] Rumelhart, D E., Geoffrey E. H., Williams, R. J. 1986. Learning Internal Representations by Error Propagation".
- [111] T. Chio, G. Huang and S. Zhou, "Application of Direct Metal Laser Sintering to Waveguide-Based Passive Microwave Components, Antennas, and Antenna Arrays," in Proceedings of the IEEE, vol. 105, no. 4, pp. 632-644, April 2017. doi: 10.1109/JPROC.2016.2617870.
- [112] O. A. Peverini et al., "Selective Laser Melting Manufacturing of Microwave Waveguide Devices," in Proceedings of the IEEE, vol. 105, no. 4, pp. 620-631, April 2017. doi: 10.1109/JPROC.2016.2620148.
- [113] G. Huang, S. Zhou, C. Sim, T. Chio and T. Yuan, "Lightweight Perforated Waveguide Structure Realized by 3-D Printing for RF Applications," in IEEE Transactions on Antennas and Propagation, vol. 65, no. 8, pp. 3897-3904, Aug. 2017. doi: 10.1109/TAP.2017.2715360.
- [114] E. A. Rojas-Nastrucci, J. Nussbaum, T. M. Weller and N. B. Crane, "Metallic 3D printed Ka-band pyramidal horn using binder jetting," 2016 IEEE MTT-S Latin

- America Microwave Conference (LAMC), Puerto Vallarta, 2016, pp. 1-3. doi: 10.1109/LAMC.2016.7851297.
- [115] Zhang, B., Guo, Y. X., Sun, H., & Wu, Y. (2018). Metallic, 3D-Printed, K-Band-Stepped, Double-Ridged Square Horn Antennas. Applied Sciences, 8(1), 33.
- [116] Mahouti P., Güneş F., Belen M. A., Çalışkan A., "A Novel Design of Non-Uniform Reflectarrays with Symbolic Regression and its Realization using 3-D Printer," Applied Computational Electromagnetics Society Journal.
- [117] Nayeri P., Liang M., R. A., Sabory-Garcia M. Tuo, Yang F., Gehm M., Xin H., and Elsherbeni A. Z., "3D printed dielectric reflectarrays: Low-cost high-gain antennas at submillimeter waves," IEEE Trans. Antennas Propag., Vol. 62, No. 4, 2000–2008, Apr. 2014.
- [118] Mirzaee, M., Noghanian S., Wiest L., and Chang Y., "Developing flexible 3D printed antenna using conductive ABS materials," IEEE International Symposium on Antenna and Propagation and North American Radio Science Meeting 2015, 1308–1309, Jul. 2015.
- [119] Ahn, B. Y., E. B. Duoss, M. J. Motala, X. Guo, S.-I. Park, Y. Xiong, J. Yoon, R. G. Nuzzo, J. A. Rogers, and J. A. Lewis, "Omnidirectional printing of flexible, stretchable, and spanning silver microelectrodes," Science, Vol. 323, No. 5921, 1590–1593, Mar. 2009.
- [120] Mahouti P., , Belen M. A., Güneş F., Yurt R., 2019. Design and Realization of Multilayered Cylindrical Dielectric Lens Antenna Using 3D Printing Technology, Microwave and Optical Technology Letters
- [121] Belen M. A., Mahouti P., 2018.Design and realization of quasi Yagi antenna for indoor application with 3D printing technology. Microwave and Optical Technology Letters, 60:2177–2181. https://doi.org/10.1002/mop.31319.
- [122] Mahouti, P., 3 Boyutlu Yazıcı Teknolojisi ile Bir Mikroşerit Yama Antenin Maliyet Etkin Üretimi, Journal of Engineering Sciences and Design, 2019, (in Turkish).
- [123] Toy Y. C., Mahouti P., Güneş F. and Belen M. A., "Design and manufactering of an X-band horn antenna using 3-D printing technology," 2017 8th International Conference on Recent Advances in Space Technologies (RAST), Istanbul, 2017, pp. 195-198.
- [124] Belen M. A., Mahouti P., Realization of Dielectric Sheets for Gain Improvement of Ultra-Wideband Horn Antennas Using 3D Printer Technology, Applied Computational Electromagnetics Society Journal, 34, 5, 2019,
- [124] Travelling Wave Broadband, and Frequency Independent Antennas, EE-4382/5306-Antenna Engineering, http://emlab.utep.edu/ee4382_AntennaEngineering/Topic%207%20-traveling%20Wave%20and%20Frequency%20Independent%20Antennas.pdf, (2018, August 29)

- [125] Güneş F, Mahouti P, Demirel S, Belen MA, Uluslu A. Cost-effective GRNN-based modeling of microwave transistors with a reduced number of measurements. Int J Numer Modell Electron Networks Devices Fields. 2015.
- [126] https://www.cst.com/solutions/article/antenna-radiation-efficiency-tool-antenna-magus (2020, July 15).
- [127] https://www.lpkf.com/products/rapid-pcb-prototyping/circuit-board-plotter/protomat-s63.htm (2020, October 12).
- [128] LB8180, 0.8-18 GHz broadband horn antenna, 2017, August: http://www.ainfoinc.com/en/p_ant_h_brd.asp (2020, November 18).
- [129] Güneş F., Sharipov Z., Belen M. A., Mahouti P., "GSM filtering of horn antennas using modified double square frequency selective surface", Int J RF Microw Comput Aided Eng. vol.27, 2017.
- [130] Esquius-Morote M., Fuchs B., Zürcher J.-F., and Mosig J.R., "Novel thin and compact H-plane SIW horn antenna", IEEE Transactions on Antennas and Propagation, vol.61(6), 2013.
- [131] Collado A. and Georgiadis A., "24 GHz substrate integrated waveguide (SIW) rectenna for energy harvesting and wireless power transmission," IEEE MTT-S International Microwave Symposium Digest (MTT), Seattle, WA, 2013, pp. 1-3, 2013 doi: 10.1109/MWSYM.2013.6697772
- [132] Sabri L., Amiri N., Amiri K. Forooraghi, "Dual-Band and Dual-Polarized SIW-Fed Microstrip Patch Antenna," IEEE Antennas and Wireless Propagation Letters, vol. 13, pp. 1605-1608, 2014. doi: 10.1109/LAWP.2014.2339363
- [133] Cheng T., Cheng W. Jiang, Gong S., Yu Y., "Broadband SIW Cavity-Backed Modified Dumbbell-Shaped Slot Antenna," IEEE Antennas and Wireless Propagation Letters, vol. 18(5), pp. 936-940, 2019. doi: 10.1109/LAWP.2019.2906119
- [134] Jiang W., Huang K., Liu C., "Ka-Band Dual-Frequency Single-Slot Antenna Based on Substrate Integrated Waveguide", IEEE Antennas and Wireless propagation letters, vol. 17(2), 2018.
- [135] Wu Y., Ding K., Zhang B., Wu D., Li J., "SIW-tapered slot antenna for broadband MIMO Applications", IET Microw. Antennas Propag., vol. 12(4), pp. 612-616, 2018.
- [136] Zhang, S., Arya, R.K., Pandey, S., et al.: '3D-printed planar graded index lenses', Microw. Antennas Propag., 2016, 10, (13), pp. 1411–1419, doi: 10.1049/ietmap.2016.0013.
- [137] Türk, A. S., Keskin, A. K., Şentürk, M. D., "Dielectric loaded TEM horn-fed ridged horn antenna design for ultrawideband ground-penetrating impulse radar", Turkish J Elec Eng & Comp Sci. 23: 1479 1488, 2015.
- [138] Bauerle, R. J., Schrimpf, R., Gyorko, E., Henderson, J., "The Use of a Dielectric Lens to Improve the Efficiency of a Dual-Polarized Quad-Ridge Horn from 5 to 15 GHz", IEEE Transactions on Antennas and Propagation, Vol. 57, No. 6, June 2009.

- [139] Jinpil Tak, Do-Gu Kang, and Jaehoon Choi, "A Lightweight Waveguide Horn Antenna Made Via 3D Printing And Conductive Spray Coating", Microwave And Optical Technology Letters / Vol. 59, No. 3, March 2017
- [140] Mohd Fadzil Ain, Othman Ali, and Zainal Arifin Ahmad, "Hybrid Dielectric Resonator Integrated Pyramidal Horn Antenna", Microwave And Optical Technology Letters / Vol. 55, No. 6, June 2013
- [141] Belen M. A., Güneş F., Mahouti P., and Belen A., "UWB Gain Enhancement of Horn Antennas Using Miniaturized Frequency Selective Surface", ACES IOURNAL, Vol. 33, No. 9, September 2018.
- [142] Pozar DM, Metzler TA. Analysis of a reflect array antenna using microstrip patches of variable size. Electron Lett. 1993;27:657-658.
- [143] M. Moeini-Fard, M. Khalaj-Amirhosseini, "Nonuniform Reflect-Array Antennas", International Journal of RF and Microwave Computer-Aided Engineering/Vol. 22, No. 5, September 2012
- [144] R. Shamsaee Malfajani and Zahra Atlasbaf, "Design and Implementation of a Dual-Band Single Layer Reflectarray in X and K Bands", IEEE transactions on antennas and propagation, vol. 62, no. 8, 2014
- [145] Fan Yang, Ruyuan Deng, Shenheng Xu, and Maokun Li, "Design and Experiment of a Near-Zero-ThicknessHigh-Gain Transmit-Reflect-Array Antenna Using Anisotropic Metasurface", IEEE transactions on antennas and propagation, vol. 66, no. 6,2018
- [146] Veluchamy L, Alsath MGN, Selvan KT. Design and evaluation of a wideband reflectarray antenna using cross dipole with double-ring elements. Int J RF Microw Computer Aided Eng. 2019;e21865. https://doi.org/10.1002/mmce. 21865
- [147] Chaharmir MR, Shaker J, Legacy H. Broadband design of a single layer reflectarray using multi cross loop elements. IEEE Trans Antennas Propag. 2009;57:3363-3366

PUBLICATION FROM THE THESIS

Papers

- **1.** Belen A, Günes,F, Mahouti P, Tari Ö., Gain Enhancement of a Traditional Horn Antenna using 3D Printed Square- Shaped Multi-layer Dielectric Lens for X band Application The Applied Computational Electromagnetics Society, (Accepted)
- **2.** Belen A, Günes,F, Mahouti P, Design Optimization of a Dual Band Microstrip SIW Antenna Design and Performance Enhancement Using Differential Evolutional Algorithm The Applied Computational Electromagnetics Society, vol 35 (7),778-783, 2020
- **3.** Belen A, Günes, F, Belen MA., Mahouti P, 2020. 3D Printed Wideband Flat Gain Multilayer Non-Uniform Reflect Array Antenna for X Band Applications International Journal of Numerical Modelling: Electronic Networks, Devices and Fields, https://doi.org/10.1002/jnm.2753
- **4.** Belen A, Günes, F, Mahouti P, Palandöken M. 2019. A Novel Design of High Performance multilayered cylindrical dielectric lens antenna using 3D printing technology. Int. J. RF Microwave Computer Aided Eng. 2019;e21988.https://doi.org/10.1002/mmce.21988
- **5.** Günes, F, Belen A, Belen MA. 2019. Microstrip tapered traveling wave antenna for wide range of beam scanning in X- and Ku-bands. Int. J. RF Microw Computer Aided Eng. 2019;29: e21771. https://doi.org/10.1002/mmce.21771
- **6.** Belen A, Günes, F Design And Realization of Dual Band Microstrip SIW Antenna, Sigma J Eng & Nat Sci 38 (1), 2020, 305-310

Books

1. Aysu BELEN, Filiz GÜNEŞ, Reflection Characteristics of Microstrip Reflectarray Antennas via The Full Wave EM Simulation Based Artificial Neural Networks, 143-156, Academic Studies in Engineering – II, Gece Kitaplığı / Gece Publishing Editor Prof. Dr. Reyhan İrkin, ISBN • 978-625-7884-57-0, Baskı & Cilt / Printing & Volume Sertifika / Certificate No: 47083